Journal of Dynamics and Differential Equations (2021) 33:1917–1957
https://doi.org/10.1007/s10884-020-09878-9

Stability and Double-Hopf Bifurcations of a Gause–Kolmogorov-Type Predator–Prey System with Indirect Prey-Taxis

Wenjie Zuo[1] · **Yongli Song**[2]

Received: 17 March 2020 / Revised: 16 July 2020 / Published online: 7 August 2020

Abstract

In this paper, we deal with the Gause–Kolmogorov-type predator–prey system with indirect prey-taxis, which means that directional movement of predators is stimulated by some chemicals emitted by preys. The existence of the positive equilibrium, the effect of the indirect prey-taxis on the stability and the related bifurcations are investigated. The critical values for the occurrence of the Hopf bifurcation, Turing bifurcation, Turing–Hopf bifurcation and double-Hopf bifurcation are explicitly determined. An algorithm for calculating the normal form of the double-Hopf bifurcation for the non-resonance and weak resonance is derived. Moreover, we apply the theoretical results to the system with Holling-II type functional response, the stable region and the bifurcation curves are completely determined in the plane of the indirect prey-taxis and self saturation coefficient. The dynamical classification near the double-Hopf bifurcation point is explicitly determined. In the neighborhood of the double-Hopf bifurcation, there are stable spatially homogeneous/inhomogeneous periodic solutions, stable spatially inhomogeneous quadi-periodic solutions and the pattern transitions from one spatial–temporal patterns to another one with the changes of the indirect taxis and semi saturation coefficients. The results show that spatially inhomogeneous Hopf bifurcations are induced by an indirect prey-taxis parameter $\chi > 0$, which is impossible for the reaction–diffusion predator–prey model with a direct prey-taxis.

Keywords Predator–prey model · Indirect prey-taxis · Stability · Double-Hopf bifurcation · Turing–Hopf bifurcation

Partially supported by the NSFC of China (Nos. 11971143, 11671236), Shandong Provincial Natural Science Foundation (No. ZR2019MA006), the Fundamental Research Funds for the Central Universities (No. 19CX02055A) and Natural Science Foundation of Zhejiang Province of China (No. LY19A010010).

✉ Yongli Song
songyl@hznu.edu.cn

1 College of Science, China University of Petroleum (East China), Qingdao 266580, China

2 Department of Mathematics, Hangzhou Normal University, Hangzhou 311121, China

1 Introduction

Since the pioneer work of Lotka [32] and Volterra [50], predator–prey interactions have been one of the hottest topics in mathematics and ecology and exhibited the rich biodiversity of ecosystem [3]. Spatiotemporal heterogeneity plays an important role in ecological systems, directly accounting for ecosystem biodiversity and species interactions. The reaction–diffusion models including taxis terms provide effective theoretical and practical tools in describing the spatiotemporal heterogeneity in ecosystems [6,7,29,33,34,46]. The prey-taxis describes active movement of predators towards the area of higher prey density, which was first observed in the experiment and treated as biased random walks by Karevia and Odell [25].

In view of the random diffusion of predator and prey and biased random walks to prey, a general reaction–diffusion equation with direct prey-taxis is the following form:

$$\begin{cases} \frac{\partial N}{\partial t} = Nf(N) - Pg(N) + \delta_N \triangle N, \ \ x \in \Omega, \ t > 0, \\ \frac{\partial P}{\partial t} = \gamma P g(N) - mP + \nabla \cdot (-\chi(P)\nabla N + \delta_P \nabla P), \ \ x \in \Omega, \ t > 0, \end{cases} \tag{1.1}$$

where $N(x,t),\ P(x,t)$ are the densities of prey and predator populations at space x and time t, $Pg(N)$ denotes the inter-specific interaction, $f(N)$ is the per capita growth rate of the prey population in the absence of predator. m is the mortality rate of the predator population. γ is the conversion coefficient. In particular, $g(N)$ is the functional response which reflects the intake rate of predators to preys. $\delta_N,\ \delta_P$ are the diffusion coefficients of the prey and predator. $\nabla \cdot (-\chi(P)\nabla N)$ denotes the tendency of predator moving upward or downward the prey gradient direction. The existence and uniqueness of weak solutions of system (1.1) were obtained by [2]. Tao [44] investigated the existence and uniqueness of classical solutions of system (1.1) in a smooth bounded domain $\Omega \subset R^n,\ 1 \le n \le 3$. Pattern formation induced by prey-taxis was studied for different functional responses in [29]. The existence, bifurcation of nonconstant steady state and pattern formations of system (1.1) are investigated in [52]. Wu et al. [53] focused on a more general form of system (1.1) and obtained the global existence and boundness of the solutions. Wang et al. [51] studied the existence and boundedness of the solutions of the three-species predator–prey model with two prey-taxis in bounded domain of arbitrary spatial domain. Yousefnezhad et al. [54] studied the global stability of the constant positive equilibrium of a predator–prey system with prey-taxis and special functional responses by constructing a Lyapunov function. The existence of nonconstant steady state and Turing instability induced by direct prey-taxis has also been widely investigated in the literatures (see [5,24,27,30,55,56]), which show that the prey-taxis term can destabilize the constant equilibrium.

Direct taxis models as (1.1) to simulate the active movement of predators to preys are fraught since such models can not result in stable spatially heterogeneous dynamical behaviors in the absence of nonlinear terms, illustrated in [4,19,47]. Instead of a direct influence of prey-taxis and assuming that the taxis is stimulated by some chemicals that are continuously emitted by prey (e.g., odour, pheromones, exometabolites), the predator–prey model with the indirect prey-taxis has attracted the great attention of the researchers. Compared with the direct prey-taxi, there is a little work on the predator–prey system with indirect prey-taxis.

It has been shown that intensive indirect prey-taxis results in the spatial heterogeneity in the predator–prey models even in the absence of predator's reproduction and mortality processes [4,9,45]. Recently, Tyutyunov et al. [49] investigated the influence of the indirect prey-taxis on the dynamics for the diffusive Gause–Kolmogorov-type predator–prey model, where the predator ability to pursue the prey is modelled by the Patlak–Keller–Segel taxis model and the movement velocities of predators are proportional to the gradients of specific cues emitted by the prey population. And it has been shown that the prey-taxis destabilizes the constant steady state and induces Hopf bifurcation. Tyutyunov et al. [48] considered the indirect prey-taxis model based on the Rosenzweig–MacArthur predator–prey model with Allee effect in predator population growth. They found that the indirect prey-taxis activity of the predator can destabilize both the stationary and periodic spatially-homogeneous regimes of the species coexistence. The results in [48,49] are mainly based on the numerical investigation and the assumption. More recently, Ahn et al. [1] proved the global existence and uniform boundedness of solutions of system (1.2) with indirect taxis in any spatial domain and the global stability of semi-trivial equilibrium, And the simulations reveal that indirect prey-taxis can result in complex spatial patterns.

In the present paper, we consider the following Gause–Kolmogorov-type predator–prey system with indirect prey-taxis as follows:

$$\begin{cases} \frac{\partial N}{\partial t} = Nf(N) - Pg(N) + \delta_N \triangle N, \;\; x \in \Omega, \; t > 0, \\ \frac{\partial P}{\partial t} = \gamma P g(N) - mP + \nabla \cdot (-\chi P \nabla S + \delta_P \nabla P), \;\; x \in \Omega, \; t > 0, \\ \frac{\partial S}{\partial t} = \xi N - \eta S + \delta_S \triangle S, \;\; x \in \Omega, \; t > 0, \\ \frac{\partial N}{\partial \nu} = \frac{\partial P}{\partial \nu} = \frac{\partial S}{\partial \nu} = 0, \;\; x \in \partial\Omega, \; t > 0, \\ N(x,0) = N_0(x) \geq 0, \; P(x,0) = P_0(x) \geq 0, \; S(x,0) = S_0(x) \geq 0, \; x \in \Omega, \end{cases} \tag{1.2}$$

where $S(x,t)$ is the taxis stimulus concentration, δ_S is the constant diffusion coefficient of stimulus, χ is the taxis coefficient of the predator population. When $\chi = 0$, there is no indirect prey-taxis. Generally, $\chi > 0$ (known as the attractive taxis), which implies that the prey-taxis movements of predator density are positively stimulated by some chemical emitted by the prey and show the tendency to the high prey area. When the predator may retreat from high prey area, χ can be negative (known as the repulsive taxis), which occurs in the case when the prey act anti-predator defensive behaviors and show chemical defences [31]. Other parameters are as the same as system (1.1). Here, we choose $\Omega = (0, l\pi)$ for simplicity and convenience in computing the normal forms and carrying out the numerical simulations. ν is the outer normal direction. The zero-flux boundary condition is imposed to imply that the system is close to the exterior environment.

The primary purpose in this paper is to investigate mathematically what interesting dynamical behaviors for system (1.2). Especially, we investigate the occurrence of the codimension-two double-Hopf bifurcation and Turing–Hopf bifurcation and determine the dynamical classification near the double-Hopf bifurcation by calculating the normal form of the double-Hopf bifurcation. System (1.2) has been proposed in [49], however, to the best of our knowledge, the study for the stability and codimension-two bifurcation is the first mathematical investigation.

As we all know, the codimension-one Hopf bifurcation and Turing bifurcation have been extensively studied in various reaction–diffusion systems (e.g. [8,17,23,40,49,57]). However, the interactions of double-Hopf bifurcations may generate spatially homogeneous and nonhomogeneous periodic solutions, quasi-periodic solutions, coexisting of several periodic solutions [13,20,21]. Interactions of Turing and Hopf bifurcations may generate spatiotemporal periodic pattern, bistability between spatial and temporal patterns [38,40,42,43]. Following the outstanding work of Faria [16,18], the general frame of calculating the normal forms of double-Hopf bifurcations has been derived by Jiang and Song [22] for the delay differential equations under the case of non-resonance and weak resonance and by Du et al. [13] for the reaction–diffusion with delay, where is no prey-taxis, and by Song et al. [39] for the resource-consumer model with random and memory-based diffusions.

In comparison with other existing results, we roughly summarize our main results as follows:

- The spatially inhomogeneous Hopf bifurcations induced by the indirect prey-taxis for the predator–prey model are found.
- Taking the indirect taxis coefficient and other parameter as the bifurcation parameters, we mathematically investigate the existence of double-Hopf bifurcations and Turing–Hopf bifurcations of system (1.2), which reflect that indirect prey-taxis can bring about rich dynamical behaviors.
- An algorithm for calculating the normal form of the double-Hopf bifurcation for the non-resonance and weak resonance is derived, which guarantees the exact regional divisions with different dynamics near double-Hopf bifurcation points.
- Our theoretical results are applied to the predator–prey system (1.2) with Holling-II functional response and some interesting pattern formations are illustrated.

We would like to mention that spatially inhomogeneous Hopf bifurcations do not occur for the reaction–diffusion predator–prey model with a direct prey-taxi like (1.1) when $\chi > 0$, and here it is shown that an indirect prey-taxi can generate spatially inhomogeneous Hopf bifurcations. The spatially inhomogeneous Hopf bifurcations are also proved in [31] for the attraction-repulsion Keller–Segel system. The mechanism there is to have both attractive and repulsive chemotaxis, while the mechanism here is to have indirect prey-taxi. Both of them need three equations. However, when the delay is involved into the diffusion terms, spatially inhomogeneous Hopf bifurcations can occur even for the single population model with memory-based diffusion [36,37,41]. In [37], the authors first proposed this spatial memory model and it has been shown that the delay-induced spatially inhomogeneous Hopf bifurcations are always unstable. However, the delay-induced stable spatially inhomogeneous Hopf bifurcations are possible in the models proposed in [36,41]. In [41], the mechanism of spatially inhomogeneous Hopf bifurcations comes from the interaction of the memory delay and the nonlocal reaction, while in [36], it comes from the interaction of the memory delay and maturation delay. For classical Keller–Segel equation with logistic growth, spatially inhomogeneous periodic orbits are also found, but which are not the results of Hopf bifurcation from the positive constant equilibrium [15,35].

The rest of this article is as follows. In Sect. 2, we investigate the stability of the positive equilibrium and existence of spatially homogeneous and nonhomogeneous Hopf bifurcations and Turing bifurcations, and the critical values of the double-Hopf bifurcation and Turing–Hopf bifurcation points are explicitly obtained. Besides, our results are applied to the system (2.12) with Holling-II functional response and the corresponding results are derived. In Sect. 3, the normal form of double-Hopf bifurcation for a general reaction–diffusion system with indirect prey-taxis is derived and rich dynamical behaviors near the double-Hopf bifurcation points are discussed. In Sect. 4, numerical simulations are illustrated to verify and expand our theoretical results and complex spatial patterns are exhibited. Conclusion and further discussion are given in Sect. 5.

2 Stability and Bifurcation Analysis

In this article, we further assume the absence of the Allee effect in the prey population. Moreover, the functional response of predators is only prey-dependent, which implies that $f(N)$ and $g(N)$ satisfy the following conditions formulated by Kolmogorov [26]:

$(H1)$ $f(0) > 0,$ $f'_N < 0$ and there exists a constant $K > 0$ such that $f(K) = 0$;

$(H2)$ $g(0) = 0,$ $g'_N > 0$ and there exists a constant $N_2^* > 0$ such that $g(N_2^*) = \frac{m}{\gamma}$.

It is shown that the system (1.2) has the zero equilibrium $E_0(0, 0, 0)$ and the boundary equilibrium $E_1(K, 0, \frac{\xi K}{\eta})$ (extinction of predator) and the unique positive equilibrium $E_2(N_2^*, P_2^*, S_2^*)$ (coexistence of prey and predator), where

$$N_2^* = g^{-1}\left(\frac{m}{\gamma}\right), \ P_2^* = \frac{N_2^* f(N_2^*)}{g(N_2^*)} = \frac{\gamma N_2^* f(N_2^*)}{m}, \ S_2^* = \frac{\xi N_2^*}{\eta}. \tag{2.1}$$

The corresponding ordinary differential equation of system (1.2) is as follows:

$$\begin{cases} \frac{dN}{dt} = Nf(N) - Pg(N), \\ \frac{dP}{dt} = \gamma P g(N) - mP, \\ \frac{dS}{dt} = \xi N - \eta S. \end{cases} \tag{2.2}$$

From [49], we have the following result:

Lemma 2.1 [49] *System (2.2) has a unique positive equilibrium $E_2(N_2^*, P_2^*, S_2^*)$ defined by (2.1), which is locally asymptotically stable if $f(N_2^*) - P_2^* g'(N_2^*) + N_2^* f'(N_2^*) < 0$ and unstable if $f(N_2^*) - P_2^* g'(N_2^*) + N_2^* f'(N_2^*) > 0$. And system (2.2) undergoes a Hopf bifurcation at $E_2(N_2^*, P_2^*, S_2^*)$ when $f(N_2^*) - P_2^* g'(N_2^*) + N_2^* f'(N_2^*) = 0$.*

Through this section, we assume the following condition holds:

$(H3)$ $f(N_2^*) - P_2^* g'(N_2^*) + N_2^* f'(N_2^*) \leq 0$.

The linearization of the system (1.2) at $E_2(N_2^*, P_2^*, S_2^*)$ is as follows:

$$\begin{pmatrix} \frac{\partial N}{\partial t} \\ \frac{\partial P}{\partial t} \\ \frac{\partial S}{\partial t} \end{pmatrix} = D \begin{pmatrix} \triangle N \\ \triangle P \\ \triangle S \end{pmatrix} + A \begin{pmatrix} N \\ P \\ S \end{pmatrix},$$

where

$$D = \begin{pmatrix} \delta_N & 0 & 0 \\ 0 & \delta_P & -\chi P_2^* \\ 0 & 0 & \delta_S \end{pmatrix},$$

and

$$A = \begin{pmatrix} a_{11} & -g(N_2^*) & 0 \\ \gamma P_2^* g'(N_2^*) & \gamma g(N_2^*) - m & 0 \\ \xi & 0 & -\eta \end{pmatrix} = \begin{pmatrix} a_{11} & -\frac{m}{\gamma} & 0 \\ \gamma P_2^* g'(N_2^*) & 0 & 0 \\ \xi & 0 & -\eta \end{pmatrix},$$

where $a_{11} = f(N_2^*) - P_2^* g'(N_2^*) + N_2^* f'(N_2^*) \leq 0$.

It is well-known that the eigenvalue problem

$$-\triangle u(x) = \mu u(x), \quad x \in (0, l\pi),$$
$$u_x(0) = u_x(l\pi) = 0,$$

has the eigenvalues $\mu_n = \frac{n^2}{l^2}$, $n = 0, 1, 2, \ldots$, with the corresponding normalized eigenfunctions

$$\beta_n^{(j)}(x) = r_n(x)e_j, \; r_n(x) = \frac{\cos \frac{nx}{l}}{\| \cos \frac{nx}{l} \|_{2,2}} = \begin{cases} \frac{1}{\sqrt{l\pi}}, & n = 0, \\ \sqrt{\frac{2}{l\pi}} \cos \frac{nx}{l}, & n \neq 0. \end{cases} \tag{2.3}$$

The characteristic equations corresponding to the positive equilibrium $E_2(N_2^*, P_2^*, S_2^*)$ are

$$\lambda^3 + P(\chi, n)\lambda^2 + Q(\chi, n)\lambda + R(\chi, n) = 0, \tag{2.4}$$

where

$$\begin{aligned} P(\chi, n) &= (\delta_N + \delta_S + \delta_P)\left(\frac{n}{l}\right)^2 + \eta - a_{11}, \\ Q(\chi, n) &= (\delta_N\delta_S + (\delta_S + \delta_N)\delta_P)\left(\frac{n}{l}\right)^4 + (\eta(\delta_N + \delta_P) - (\delta_S + \delta_P)a_{11})\left(\frac{n}{l}\right)^2 \\ &\quad - \eta a_{11} + mP_2^* g'(N_2^*), \\ R(\chi, n) &= \delta_N\delta_S\delta_P\left(\frac{n}{l}\right)^6 + (\delta_N\delta_P\eta - a_{11}\delta_S\delta_P)\left(\frac{n}{l}\right)^4 + \eta m P_2^* g'(N_2^*) \\ &\quad + \left(-\eta\delta_P a_{11} + mP_2^* g'(N_2^*)\delta_S + \frac{m\xi}{\gamma}\chi P_2^*\right)\left(\frac{n}{l}\right)^2. \end{aligned} \tag{2.5}$$

2.1 Stability, Hopf and Double-Hopf Bifurcations

In this section, we consider the stability and Hopf bifurcation of the system (1.2) by analyzing the characteristic values. By the Routh–Hurwitz criterion, $E_2(N_2^*, P_2^*, S_2^*)$ is locally asymptotically stable if and only if for all $n = 0, 1, 2, \ldots,$

$$\triangle_{1n} > 0, \; \triangle_{2n} > 0, \; \triangle_{3n} > 0,$$

where

$$\begin{aligned} \triangle_{1n} &= P(\chi, n) = (\delta_N + \delta_S + \delta_P)\left(\frac{n}{l}\right)^2 + \eta - a_{11} > 0, \\ \triangle_{2n} &= \begin{vmatrix} P(\chi, n) & 1 \\ R(\chi, n) & Q(\chi, n) \end{vmatrix} = P(\chi, n)Q(\chi, n) - R(\chi, n) \\ &= b_1\left(\frac{n}{l}\right)^6 + b_2\left(\frac{n}{l}\right)^4 + b_3\left(\frac{n}{l}\right)^2 - \frac{m\xi}{\gamma}\chi P_2^*\left(\frac{n}{l}\right)^2 + b_4, \\ \triangle_{3n} &= \begin{vmatrix} P(\chi, n) & 1 & 0 \\ R(\chi, n) & Q(\chi, n) & P(\chi, n) \\ 0 & 0 & R(\chi, n) \end{vmatrix} = R(\chi, n)\triangle_{2n}, \end{aligned}$$

with

$$\begin{aligned} b_1 &= (\delta_s + \delta_N)\delta_P^2 + \delta_S^2(\delta_P + \delta_N) + \delta_N^2(\delta_S + \delta_P) + 2\delta_N\delta_S\delta_P > 0, \\ b_2 &= \eta(\delta_N^2 + \delta_P^2 + 2\delta_P(\delta_S + \delta_N) + 2\delta_S\delta_N) \\ &\quad - a_{11}(\delta_S^2 + \delta_P^2 + 2((\delta_N + \delta_S)\delta_P + \delta_N\delta_S)) > 0, \\ b_3 &= a_{11}^2(\delta_S + \delta_P) - 2a_{11}\eta(\delta_S + \delta_P) - 2a_{11}\eta\delta_N + \eta^2(\delta_N + \delta_P) \\ &\quad + mP_2^* g'(N_2^*)(\delta_N + \delta_P) > 0, \\ b_4 &= a_{11}^2\eta - a_{11}\eta^2 - a_{11}mP_2^* g'(N_2^*) \begin{cases} = 0, & a_{11} = 0, \\ > 0, & a_{11} < 0. \end{cases} \end{aligned} \tag{2.6}$$

Clearly, the sign of $\triangle_{3n}$ agrees with $\triangle_{2n}$ since $R(\chi, n) > 0$ for all $n \in N_0 \triangleq \{0, 1, 2, \ldots\}$. Thus, the stability of $E_2(N_2^*, P_2^*, S_2^*)$ and the existence of Hopf bifurcation are determined only by the sign of $\triangle_{2n}$. It is easy to check that, when $a_{11} < 0$, system (1.2) has no Hopf bifurcation for any $\chi \leq 0$ since $\triangle_{2n} > 0$ for $n \in N_0$. Thus, when $a_{11} < 0$, we can obtain the existence of Hopf bifurcation only when $\chi > 0$. In this case, $\lambda = 0$ is not a root of the characteristic Eq. (2.4).

The necessary condition for Hopf bifurcation to occur is $\triangle_{2n} = 0$ for a fixed $n \in N_0$, which is equivalent to

$$\chi \triangleq \chi_n^H = \frac{\gamma}{m\xi P_2^*}\left(b_1\left(\frac{n}{l}\right)^4 + b_2\left(\frac{n}{l}\right)^2 + b_3 + b_4\left(\frac{l}{n}\right)^2\right) > 0,\ n = 1, 2, \ldots, \tag{2.7}$$

or

$$a_{11} = 0,\ n = 0.$$

Remark 2.1 The Hopf bifurcation curve $a_{11} = f(N_2^*) - P_2^* g'(N_2^*) + N_2^* f'(N_2^*) = 0,\ n = 0$ of the diffusive system (1.2) is exactly the Hopf bifurcation of the corresponding ODE (2.2).

Hence, for fixed $n \in \{1, 2, \ldots\}$, Eq. (2.4) has a pair of purely imaginary roots,

$$\lambda_n = \pm i\omega_n = \pm i\sqrt{Q(\chi, n)} \text{ at } \chi = \chi_n^H. \tag{2.8}$$

Next, we verify that the transversality condition holds.

Taking the derivative of both sides of Eq. (2.4) with respect to χ at $\chi = \chi_n^H$, we have that,

$$\frac{d\lambda}{d\chi}(3\lambda^2 + 2\lambda P(\chi, n) + Q(\chi, n))\bigg|_{\chi=\chi_n^H} = -\frac{m\xi}{\gamma} P_2^* \left(\frac{n}{l}\right)^2,$$

which implies that

$$Re\left(\frac{d\lambda}{d\chi}\right)^{-1}\Bigg|_{\chi=\chi_n^H} = -\left.\frac{\gamma Re(3\lambda^2 + 2\lambda P(\chi, n) + Q(\chi, n))}{\xi m P_2^* \left(\frac{n}{l}\right)^2}\right|_{\chi=\chi_n^H} = \frac{2\gamma Q(\chi, n)}{m\xi P_2^* \left(\frac{n}{l}\right)^2} > 0.$$

Thus, $\left.\frac{dRe\lambda}{d\chi}\right|_{\chi=\chi_n^H} > 0$ since the sign of $Re\left(\frac{d\lambda}{d\chi}\right)^{-1}$ is consistent with the sign of $\frac{dRe\lambda}{d\chi}$.

In the sequel, we show the monotonicity of the critical values χ_n^H with respect to n.

Lemma 2.2 *Let x_0 be a unique positive root of the cubic equation $2b_1x^3 + b_2x^2 - b_4 = 0$, where b_1, b_2, b_4 are defined in (2.6). Set*

$$n_H^* = \begin{cases} [\sqrt{x_0}l], & \text{if } \chi^H_{[\sqrt{x_0}l]} \leq \chi^H_{[\sqrt{x_0}l]+1}, \\ [\sqrt{x_0}l] + 1, & \text{if } \chi^H_{[\sqrt{x_0}l]} > \chi^H_{[\sqrt{x_0}l]+1}. \end{cases} \tag{2.9}$$

Then χ_n^H is decreasing in $n \leq n_H^*$ and increasing in $n > n_H^*$. That is, $\chi^H_{n_H^*} = \min_{n\in\{1,2,\ldots\}}\{\chi_n^H\}$, where χ_n^H is defined by (2.7).

In particular, when $a_{11} = 0$, χ_n^H is increasing in n, that is, $\chi_1^H = \min_{n\in\{1,2,\ldots\}}\{\chi_n^H\}$.

Proof (i) When $a_{11} \neq 0$, let $G(x) = b_1x^2 + b_2x + b_3 + \frac{b_4}{x}$. Then $G'(x) = 2b_1x + b_2 - \frac{b_4}{x^2}$.

Clearly, $G'(x) = 0$ is equivalent to $W(x) \doteq 2b_1x^3 + b_2x^2 - b^4 = 0$.

Obviously, $W(x)$ is increasing in $(0, +\infty)$ since $b_1, b_2 > 0$ and $W(0) = -b^4 < 0$. Thus, there exists a unique $x_0 > 0$ such that $W(x_0) = 0$ and $W(x) < 0$ on $(0, x_0)$ and $W(x) > 0$ on $(x_0, +\infty)$. Since $G'(x) = W(x)/x^2$, $G(x)$ is decreasing on $(0, x_0)$ and increasing on $(x_0, +\infty)$. By the definition (2.9) of n_H^*, the result is confirmed.

(ii) When $a_{11} = 0$, $\chi_n^H = \frac{\gamma}{m\xi P_2^*}\left(b_1\left(\frac{n}{l}\right)^4 + b_2\left(\frac{n}{l}\right)^2 + b_3\right)$ is increasing in n since $b_1 > 0,\ b_2 > 0,\ b_3 > 0$. Clearly, $\chi_1^H = \min_{n\in\{1,2,\ldots\}}\{\chi_n^H\}$. □

From the analysis above, we obtain the following results:

Theorem 2.1 *Assume that the conditions* (H1)–(H3) *hold and* χ_n^H, $n = 1, 2, \ldots$, *are defined by* (2.7). *Then the following results are true:*

(I) *when* $f(N_2^*) - P_2^* g'(N_2^*) + N_2^* f'(N_2^*) < 0$ *and* $\chi \le 0$, *system (1.2) has no Hopf bifurcation;*

(II) *when* $f(N_2^*) - P_2^* g'(N_2^*) + N_2^* f'(N_2^*) < 0$ *and* $\chi > 0$, *for fixed* $\delta_N, \delta_P, \delta_S, \gamma, m, \xi, \eta, a_{11}$ *and* l,

  (i) *if for any* $j \in N_0$ *and* $j \ne n$ *such that* $\chi_j^H \ne \chi_n^H$, *system* (1.2) *undergoes spatially inhomogeneous Hopf bifurcations near the positive equilibrium* $E_2(N_2^*, P_2^*, S_2^*)$ *at* $\chi = \chi_n^H$, *and a family of spatially inhomogeneous periodic solutions bifurcate from the positive equilibrium* $E_2(N_2^*, P_2^*, S_2^*)$;

  (ii) *if there exists* $n_1, n_2, \ldots, n_s \in N_0$ *such that* $\chi_{n_1}^H = \chi_{n_2}^H = \cdots = \chi_{n_s}^H$ *and* $\chi_j^H \ne \chi_{n_1}^H$ *for* $j \ne n_1, n_2, \ldots, n_s$, *system* (1.2) *undergoes spatially inhomogeneous* $s-$*multiple Hopf bifurcations near the positive equilibrium* $E_2(N_2^*, P_2^*, S_2^*)$ *at* $\chi = \chi_{n_i}^H$, $i = 1, 2, \ldots, s$;
  In particular, if $s = 2$, 2-*multiple Hopf bifurcation is often called double-Hopf bifurcation;*

  (iii) *the positive equilibrium* $E_2(N_2^*, P_2^*, S_2^*)$ *is locally asymptotically stable for* $\chi \in [0, \chi_{n_H^*}^H)$ *and unstable for* $\chi \in (\chi_{n_H^*}^H, +\infty)$, *where* n_H^* *is defined by* (2.9);

(III) *if* $f(N_2^*) - P_2^* g'(N_2^*) + N_2^* f'(N_2^*) = 0$, *system* (1.2) *undergoes double-Hopf bifurcations near the positive equilibrium* $E_2(N_2^*, P_2^*, S_2^*)$ *at* $\chi = \chi_n^{DH}$, *where*

$$\chi_n^{DH} = \frac{\gamma}{m\xi P_2^*}\left(b_1\left(\frac{n}{l}\right)^4 + b_2\left(\frac{n}{l}\right)^2 + b_3\right) > 0,\ n = 1, 2, \ldots,$$

and $\chi_1^{DH} = \min_{n\in\{1,2,\ldots\}}\{\chi_n^{DH}\}$.

Remark 2.2 Hopf bifurcation in the predator–prey models has been widely studied in [43, 57], where Hopf bifurcation at the first critical value is always homogenous. In fact, it is exactly Hopf bifurcation of the corresponding ODE. However, the indirect-taxis-induced Hopf bifurcation at the first critical value is spatially inhomogeneous.

2.2 Turing Instability and Turing–Hopf Bifurcation

From the above analysis, we know that when $a_{11} < 0$, system (1.2) has no Turing pattern for any $\chi \ge 0$ since $\lambda = 0$ is not a root of the characteristic Eq. (2.4). Thus, we can obtain the existence of Turing bifurcation only when $\chi < 0$.

The necessary condition for Turing bifurcation to occur is $R(\chi, n) = 0$, which is equivalent to

$$\chi = \chi_n^T \triangleq -\frac{\gamma}{m\xi P_2^*}\left(\delta_N\delta_S\delta_P\left(\frac{n}{l}\right)^4 + (\delta_N\eta\delta_P - a_{11}\delta_S\delta_P)\left(\frac{n}{l}\right)^2 + \eta m P_2^* g'(N_2^*)\left(\frac{l}{n}\right)^2 - \eta\delta_P a_{11} + mP_2^* g'(N_2^*)\delta_S\right),\ n = 1, 2, \ldots. \tag{2.10}$$

Clearly, for fixed $n \in \{1, 2, \ldots\}$, Eq. (2.4) has a simple zero root at $\chi = \chi_n^T$ since $R(\chi, n) = 0,\ Q(\chi, n) > 0$. Next, we verify the transversality condition.

Taking the derivative of both sides of Eq. (2.4) with respect to χ at $\chi = \chi_n^T$, we have that,

$$\frac{d\lambda}{d\chi}(3\lambda^2 + 2\lambda P(\chi, n) + Q(\chi, n))\bigg|_{\chi=\chi_n^T} = -\frac{m\xi}{\gamma}P_2^*\left(\frac{n}{l}\right)^2,$$

which implies that

$$\left(\frac{d\lambda}{d\chi}\right)^{-1}\Bigg|_{\chi=\chi_n^T} = -\frac{\gamma(3\lambda^2 + 2\lambda P(\chi, n) + Q(\chi, n))}{\xi m P_2^*\left(\frac{n}{l}\right)^2}\Bigg|_{\chi=\chi_n^T} = -\frac{\gamma Q(\chi, n)}{m\xi P_2^*\left(\frac{n}{l}\right)^2} < 0.$$

Thus, $\frac{d\lambda}{d\chi}\Big|_{\chi=\chi_n^T} < 0$ since the sign of $\left(\frac{d\lambda}{d\chi}\right)^{-1}$ is consistent with the sign of $\frac{d\lambda}{d\chi}$.

Next, we give the monotonicity of χ_n^T on n.

Lemma 2.3 *Let x^* be a unique positive root of cubic equation*

$$2\delta_N\delta_S\delta_P x^3 + (\delta_N\eta\delta_P - a_{11}\delta_S\delta_P)x^2 - \eta m P_2^* g'(N_2^*) = 0.$$

Set

$$n_T^* = \begin{cases} [\sqrt{x^*}l], & \text{if } \chi^T_{([\sqrt{x^*}l])} \geq \chi^T_{([\sqrt{x^*}l]+1)}, \\ [\sqrt{x^*}l] + 1, & \text{if } \chi^T_{([\sqrt{x^*}l])} < \chi^T_{([\sqrt{x^*}l]+1)}. \end{cases} \tag{2.11}$$

Then χ_n^T is increasing in $n \leq n_T^*$ and decreasing in $n > n_T^*$. That is, $\chi^T_{n_T^*} = \max_{n\in\{1,2,\ldots\}}\{\chi_n^T\}$, where χ_n^T is defined by (2.10).

Proof Let

$$L(x) = \delta_N\delta_S\delta_P x^2 + (\delta_N\eta\delta_P - a_{11}\delta_S\delta_P)x + \frac{\eta m P_2^* g'(N_2^*)}{x}.$$

Clearly,

$$L'(x) = 2\delta_N\delta_S\delta_P x + (\delta_N\eta\delta_P - a_{11}\delta_S\delta_P) - \frac{\eta m P_2^* g'(N_2^*)}{x^2},$$

$$L''(x) = 2\delta_N\delta_S\delta_P + \frac{2\eta m P_2^* g'(N_2^*)}{x^3}.$$

That is, $L'(x)$ is increasing in $(0, +\infty)$ and $L'(0^+) = -\infty,\ L'(+\infty) = +\infty$. Hence, there exists a unique $x^* > 0$ such that $L'(x^*) = 0$ and $L'(x) < 0$ for $x \in (0, x^*)$ and $L'(x) > 0$ for $x \in (x^*, +\infty)$.

By the definition of n_T^*, the result is confirmed. □

In addition, it is clear that $\triangle_{1n} > 0,\ \triangle_{2n} > 0$ when $\chi < 0,\ a_{11} \le 0$. Hence, the positive equilibrium E_2 is unstable only when $R(\chi, n) < 0$, which is equivalent to

$$\chi < \max_{n\in N}\{\chi_n^T\} = \chi_{n_T^*}^T.$$

From the analysis results above and combining Lemmas 2.1 and 2.3, we have the following results:

Theorem 2.2 *Assume that the conditions* (H1)–(H3) *hold and* $\chi_n^T,\ n = 1, 2, \dots,$ *are defined by* (2.10). *Then the following results are true:*

(I) *when* $\chi \ge 0$, *system* (1.2) *has no Turing bifurcation;*
(II) *when* $\chi < 0$, *for fixed* $\delta_N,\ \delta_P,\ \delta_S,\ \gamma,\ m,\ \xi,\ \eta,\ a_{11}$ *and* l,

  (i) *if for any* $j \in N_0$ *and* $j \ne n$ *such that* $\chi_j^T \ne \chi_n^T$, *system* (1.2) *undergoes Turing bifurcations near the positive equilibrium* $E_2(N_2^*, P_2^*, S_2^*)$ *at* $\chi = \chi_n^T$*;*
  (ii) *if there exists* $n_1,\ n_2, \dots,\ n_s \in N_0$ *such that* $\chi_{n_1}^T = \chi_{n_2}^T = \dots = \chi_{n_s}^T$ *and* $\chi_j^T \ne \chi_{n_1}^T$ *for* $j \ne n_1, n_2, \dots, n_s$, *system* (1.2) *undergoes* $s-$*multiple Turing bifurcations near the positive equilibrium* $E_2(N_2^*, P_2^*, S_2^*)$ *at* $\chi = \chi_{n_1}^T$*;*
  In particular, if $s = 2$, $2-$*multiple Turing bifurcation is often called Turing–Turing bifurcation;*
  (iii) *the positive equilibrium* $E_2(N_2^*, P_2^*, S_2^*)$ *of system* (1.2) *is asymptotically stable for* $\chi_{n_T^*}^T < \chi \le 0$ *and unstable for* $\chi < \chi_{n_T^*}^T$, *where* n_T^* *is defined in* (2.11);

(III) *when* $f(N_2^*) - P_2^* g'(N_2^*) + N_2^* f'(N_2^*) = 0$, *system* (1.2) *undergoes Turing–Hopf bifurcations near the positive equilibrium* $E_2(N_2^*, P_2^*, S_2^*)$ *at* $\chi = \chi_n^{TH}$, *where*

$$\chi_{n_T^*}^{TH} = -\frac{\gamma}{m\xi P_2^*}\left(\delta_N\delta_S\delta_P\left(\frac{n_T^*}{l}\right)^4 + (\delta_N\eta\delta_P - a_{11}\delta_S\delta_P)\left(\frac{n_T^*}{l}\right)^2 + \eta m P_2^* g'(N_2^*)\left(\frac{l}{n_T^*}\right)^2 - \eta\delta_P a_{11} + mP_2^* g'(N_2^*)\delta_S\right).$$

2.3 Application to the Predator–Prey Model with Logistic Growth and Holling-II Functional Response

In this subsection, we consider the following predator–prey model with Logistic growth and Holling-II functional response:

$$\begin{cases} \frac{\partial N}{\partial t} = rN\left(1 - \frac{N}{k}\right) - \frac{\beta NP}{1+\sigma N} + \delta_N\triangle N, & x \in (0, l\pi),\ t > 0, \\ \frac{\partial P}{\partial t} = \beta\left(\frac{\gamma NP}{1+\sigma N} - \rho P\right) + \nabla\cdot(-\chi P\nabla S + \delta_P\nabla P), & x \in (0, l\pi),\ t > 0, \\ \frac{\partial S}{\partial t} = \xi N - \eta S + \delta_S\triangle S, & x \in (0, l\pi),\ t > 0, \\ N_x(x,t) = P_x(x,t) = S_x(x,t) = 0, & x = 0,\ l\pi,\ t > 0, \\ N(x,0) = N_0(x) \ge 0,\ P(x,0) = P_0(x) \ge 0,\ S(x,0) = S_0(x) \ge 0, & x \in [0, l\pi]. \end{cases} \tag{2.12}$$

Assume that

$$(A1)\quad 0 < \rho < \frac{\gamma k}{\sigma k + 1},$$

then system (2.12) has a unique positive steady state $E_2(N_2^*, P_2^*, S_2^*)$, where

$$N_2^* = \frac{\rho}{\gamma - \sigma\rho}, \; P_2^* = \frac{r\gamma}{\beta(\gamma - \sigma\rho)^2}\left(\gamma - \rho\left(\sigma + \frac{1}{k}\right)\right), \; S_2^* = \frac{\xi N_2^*}{\eta}.$$

For system (2.12), we have

$$f(N) = r\left(1 - \frac{N}{k}\right), \quad g(N) = \frac{\beta N}{1 + \sigma N}, \; m = \beta\rho,$$

and then

$$a_{11} = \rho r\left(\frac{1}{\gamma}\left(\sigma + \frac{1}{k}\right) - \frac{2}{k(\gamma - \sigma\rho)}\right), \; a_{12} = -\frac{\beta\rho}{\gamma},$$
$$a_{21} = r\left(\gamma - \rho\left(\sigma + \frac{1}{k}\right)\right), \; a_{22} = 0.$$

It is easy to verify that,

$$a_{11} < 0, \quad \text{if } \sigma \le \frac{1}{k}, \tag{2.13}$$

and when $\sigma > \frac{1}{k}$,

$$a_{11} = f(N_2^*) - P_2^* g'(N_2^*) + N_2^* f'(N_2^*) \begin{cases} < 0, & \rho > \rho_1(\sigma), \\ = 0, & \rho = \rho_1(\sigma), \\ > 0, & \rho < \rho_1(\sigma), \end{cases} \tag{2.14}$$

where

$$\rho = \rho_1(\sigma) \triangleq \frac{\gamma(k\sigma - 1)}{\sigma^2 k + \sigma} \text{ for fixed } \gamma, \; k. \tag{2.15}$$

Therefore, for the following corresponding ODE of system (2.12),

$$\begin{cases} \frac{dN}{dt} = rN\left(1 - \frac{N}{k}\right) - \frac{\beta NP}{1+\sigma N}, \\ \frac{dP}{dt} = \beta\left(\frac{\gamma NP}{1+\sigma N} - \rho P\right), \\ \frac{dS}{dt} = \xi N - \eta S, \end{cases} \tag{2.16}$$

we have the following results on the stability and Hopf bifurcation for system (2.16):

Theorem 2.3 *Assume that the condition* (A1) *holds and* $\rho = \rho_1(\sigma)$ *is defined by* (2.15). *Then the following results are true:*

(i) *if* $\sigma \le \frac{1}{k}$, *the positive steady state* $E_2(N_2^*, P_2^*, S_2^*)$ *of system* (2.16) *is always stable for any* $\rho > 0$*;*
(ii) *if* $\sigma > \frac{1}{k}$, *the positive steady state* $E_2(N_2^*, P_2^*, S_2^*)$ *of system* (2.16) *is stable for* $\rho > \rho_1(\sigma)$ *and unstable for* $\rho < \rho_1(\sigma)$*;*
(iii) *for fixed* $k, \; \gamma$ *and* $0 < \rho < \rho^*_{max}$, *where*

$$\rho^*_{max} = \frac{\sqrt{2}\gamma k}{4 + 3\sqrt{2}}, \tag{2.17}$$

system (2.16) *undergoes Hopf bifurcations at* $\sigma = \sigma_j, \; j = 1, 2$, *where* σ_1 *and* σ_2 *are two roots of* (2.15) *for fixed* ρ. *And when* $\rho^*_{max} < \rho < \frac{\gamma k}{\sigma k+1}$, *there is no Hopf bifurcation for system* (2.16).

Proof From Lemma 2.1 and (2.13), (2.14), (i) and (ii) are confirmed. Next we only verify the result (iii).

(iii) It follows from Eq. (2.15) that

$$\frac{\partial \rho_1(\sigma)}{\partial \sigma} = \frac{(-k^2\sigma^2 + 2\sigma k + 1)\gamma}{(\sigma^2 k + \sigma)^2},$$

which implies that there exists a unique $\sigma^* = \frac{1+\sqrt{2}}{k}$ such that $\frac{\partial \rho_1(\sigma)}{\partial \sigma}|_{\sigma=\sigma^*} = 0$, $\frac{\partial \rho_1(\sigma)}{\partial \sigma} > 0$ for $\sigma \in \left(\frac{1}{k}, \frac{1+\sqrt{2}}{k}\right)$ and $\frac{\partial \rho_1(\sigma)}{\partial \sigma} < 0$ for $\sigma \in \left(\frac{1+\sqrt{2}}{k}, +\infty\right)$.

Thus, for fixed $k,\ \gamma$, the function $\rho_1(\sigma)$ is increasing for $\sigma \in \left(\frac{1}{k}, \frac{1+\sqrt{2}}{k}\right)$ and decreasing for $\sigma \in \left(\frac{1+\sqrt{2}}{k}, +\infty\right)$ with respect to σ. And $\rho_1(\sigma)$ reaches its maximum value

$$\rho^*_{max} \triangleq \rho_1(\sigma^*) = \frac{\sqrt{2}\gamma k}{4 + 3\sqrt{2}}.$$

Therefor, for fixed k, γ and $\rho \in (0, \rho^*_{max}) = (0, \frac{\sqrt{2}\gamma k}{4+3\sqrt{2}})$, there exists two possible Hopf bifurcation points $\sigma_1,\ \sigma_2$ with $\sigma_1 < \frac{1+\sqrt{2}}{k} < \sigma_2$ such that

$$\rho = \frac{\gamma(k\sigma_j - 1)}{\sigma_j^2 k + \sigma_j},\ \ j = 1, 2. \tag{2.18}$$

The characteristic equation of the linearized system of (2.16) at $E_2(N_2^*, P_2^*, S_2^*)$ is

$$(\lambda + \eta)(\lambda^2 - a_{11}\lambda - a_{12}a_{21}) = 0,$$

which means that $\lambda_0 = -\eta < 0$, and

$$\lambda^2 - a_{11}\lambda - a_{12}a_{21} = 0. \tag{2.19}$$

Clearly, Eq. (2.19) has a pair of purely imaginary roots $\lambda_{1,2} = \pm i\sqrt{-a_{12}a_{21}}$ at $\sigma = \sigma_j,\ j = 1, 2$. In addition, taking the derivative of both sides of Eq. (2.19) with respect to σ at $\sigma = \sigma_j$ and combining (2.18), we have that,

$$\frac{d\lambda}{d\sigma} = \frac{\lambda \frac{\partial a_{11}}{\partial \sigma} + a_{12}\frac{\partial a_{21}}{\partial \sigma}}{2\lambda - a_{11}},$$

which implies that,

$$\begin{aligned} Re\left(\frac{d\lambda}{d\sigma}\right)^{-1}\Bigg|_{\sigma=\sigma_j} &= Re\left(\frac{\rho r\left(\lambda\left(\frac{1}{\gamma} - \frac{2\rho}{k(\gamma-\sigma\rho)^2}\right) - a_{12}\right)}{2\lambda - a_{11}}\right)\Bigg|_{\sigma=\sigma_j} \\ &= \frac{\rho r}{2}\left(\frac{1}{\gamma} - \frac{2\rho}{k(\gamma - \sigma\rho)^2}\right)\Bigg|_{\sigma=\sigma_j} \\ &= -\frac{\rho r k}{4\gamma\sigma_j}\left(\sigma_j - \frac{1+\sqrt{2}}{k}\right)\left(\sigma_j + \frac{\sqrt{2}-1}{k}\right),\ \ j = 1, 2. \end{aligned}$$

By $\sigma_1 < \frac{1+\sqrt{2}}{k} < \sigma_2$, we have that,

$$Re\left(\frac{d\lambda}{d\sigma}\right)^{-1}\Bigg|_{\sigma=\sigma_1} > 0, \quad Re\left(\frac{d\lambda}{d\sigma}\right)^{-1}\Bigg|_{\sigma=\sigma_2} < 0.$$

Hence, system (2.18) undergoes Hopf bifurcation at $\sigma_j,\ j=1,2$. Theorem 2.3 is confirmed. □

We apply the results of Sects. 2.1,2.2 to the taxis-induced predator–prey model with Logistic growth and Holling-II functional response under the condition (A1).

By Theorems 2.1, 2.2 and 2.3, we have the following results:

Theorem 2.4 *Assume that the condition* (A1) *holds and* χ_n^H, χ_n^T *are defined by* (2.7) *and* (2.10) *respectively. Then when one of the following three conditions (i)* $\sigma \le \frac{1}{k}$, *(ii)* $\rho_{max}^* < \rho < \frac{\gamma k}{\sigma k+1}$ *and* $\sigma > \frac{1}{k}$, *(iii)* $0 < \rho < \rho_{max}^*$ *and* $\sigma \in (1/k, \sigma_1) \cup (\sigma_2, \frac{\gamma k-\rho}{k\rho})$ *holds, where* $\sigma_1,\ \sigma_2$ *are homogenous Hopf bifurcation points defined by Theorem* 2.3(iii)*, the following results are true:*

- (I) *the positive equilibrium* $E_2(N_2^*, P_2^*, S_2^*)$ *is locally asymptotically stable for* $\chi \in (\chi_{n_T^*}^T, \chi_{n_H^*}^H)$ *and unstable for* $\chi \in (-\infty, \chi_{n_T^*}^T) \cup (\chi_{n_H^*}^H, +\infty)$*;*
- (II) *if for any* $j \in N_0$ *and* $j \ne n$ *such that* $\chi_j^H \ne \chi_n^H$*, system* (1.2) *undergoes spatially inhomogeneous Hopf bifurcations near the positive equilibrium* $E_2(N_2^*, P_2^*, S_2^*)$ *at* $\chi = \chi_n^H > 0$*; and if there exists* $n_1,\ n_2,\ \ldots,\ n_s$ *such that* $\chi_{n_1}^H = \chi_{n_2}^H = \cdots = \chi_{n_s}^H$ *and* $\chi_j^H \ne \chi_{n_1}^H$*, system* (1.2) *undergoes* $s-$*multiple Hopf bifurcations near the positive equilibrium* $E_2(N_2^*, P_2^*, S_2^*)$ *at* $\chi = \chi_{n_1}^H > 0$*. In particular, if* $s=2$*, system* (1.2) *undergoes double-Hopf bifurcations near the positive equilibrium* $E_2(N_2^*, P_2^*, S_2^*)$*;*
- (III) *if for any* $j \in N_0$ *and* $j \ne n$ *such that* $\chi_j^T \ne \chi_n^T$*, system* (1.2) *undergoes Turing bifurcations near the positive equilibrium* $E_2(N_2^*, P_2^*, S_2^*)$ *at* $\chi = \chi_n^T < 0$*; and if there exists* $n_1,\ n_2,\ \ldots,\ n_s$ *such that* $\chi_{n_1}^T = \chi_{n_2}^T = \cdots = \chi_{n_s}^T$ *and* $\chi_j^T \ne \chi_{n_1}^T$*, system*(1.2) *undergoes* $s-$*multiple Turing bifurcations near the positive equilibrium* $E_2(N_2^*, P_2^*, S_2^*)$ *at* $\chi = \chi_{n_1}^T > 0$*. In particular, if* $s=2$*, system* (1.2) *undergoes Turing–Turing bifurcations near the positive equilibrium* $E_2(N_2^*, P_2^*, S_2^*)$*.*

Theorem 2.5 *Assume that the condition* (A1) *holds and* χ_n^H, χ_n^T *are defined by* (2.7) *and* (2.10) *respectively. Then when* $\sigma=\sigma_1$ *or* $\sigma=\sigma_2$*, and* $0<\rho<\rho_{max}^*$*, where* $\sigma_1,\ \sigma_2$ *are homogenous Hopf bifurcation points defined by Theorem* 2.3(iii)*, system* (1.2) *undergoes double-Hopf bifurcations near the positive equilibrium* $E_2(N_2^*, P_2^*, S_2^*)$ *at* $\chi = \chi_n^H > 0,\ n=1,2,\ldots$*, and Turing–Hopf bifurcations at* $\chi=\chi_n^T<0,\ n=1,2,\ldots$*, and* $\chi_1^H = \min\limits_{n=1,2,\ldots} \{\chi_n^H\}$*.*

3 Normal Form of Double–Hopf Bifurcations on the Center Manifold

In this section, we follow the normal form theory developed in [16,42] for the reaction–diffusion system with/without delay and use the same notations as in [16,42] and derive the normal form of double-Hopf bifurcations for the non-resonance or weak resonance case. This section is also motivated by the works on the double-Hopf bifurcations in [11,12,22] for the delay differential equations without diffusion, in [13,14,39] for the reaction–diffusion with delay but without indirect prey-taxis.

3.1 Decomposition of Phase Space

From Theorem 2.2, we know that system (2.12) undergoes double-Hopf bifurcations at the interaction points (σ, χ_n^H) of two Hopf bifurcation curves near the positive steady state

$E_2(N_2^*, P_2^*, S_2^*)$. We assume that at the interaction point $(\sigma, \chi_n^H) = (\sigma^*, \chi^*)$, Eq. (2.4) has two pairs of purely imaginary roots $\pm i\omega_{n_1}, \ \pm i\omega_{n_2}$ for $n = n_1$ and $n = n_2$ with $n_1 < n_2$, respectively, which only requires that the ratio of ω_{n_1} and ω_{n_2} is not $1:1, 1:2, 1:3, 1:4$, that is non-resonance or weak resonance case. And all other eigenvalues have negative real parts. Define the real-value Sobolev space:

$$X = \{(u_1, u_2, u_3) \in (W^{2,2}(0, l\pi))^3 | \frac{\partial u_i}{\partial x} = 0, \ x = 0, l\pi, \ \ i = 1, 2, 3\}$$

with the inner product

$$[u, v] = \int_0^{l\pi} (u_1 v_1 + u_2 v_2 + u_3 v_3) dx, \ \text{for } u = (u_1, u_2, u_3), \ v = (v_1, v_2, v_3). \tag{3.1}$$

To investigate codimension-2 bifurcation, we introduce two parameters ϵ_1 and ϵ_2. Set $\epsilon_1 = \sigma - \sigma^*, \ \epsilon_2 = \chi - \chi^*$ such that $\epsilon_1 = \epsilon_2 = 0$ are double-Hopf bifurcation values. Thus, the positive equilibrium $E_2(N_2^*, P_2^*, S_2^*)$ can be written into a parameter-dependent form $E_{2\epsilon_1}(N_2^*(\epsilon_1), P_2^*(\epsilon_1), S_2^*(\epsilon_1))$ with

$$N_2^*(\epsilon_1) = \frac{\rho}{\gamma - (\sigma^* + \epsilon_1)\rho}, \ P_2^*(\epsilon_1) = \frac{r\gamma}{\beta(\gamma - (\sigma^* + \epsilon_1)\rho)^2} \left(\gamma - \rho\left(\sigma^* + \epsilon_1 + \frac{1}{k}\right)\right),$$
$$S_2^*(\epsilon_1) = \frac{\xi N_2^*(\epsilon_1)}{\eta}.$$

Letting $\tilde{N}(\cdot, t) = N(\cdot, t) - N_2^*(\epsilon_1), \ \tilde{P}(\cdot, t) = P(\cdot, t) - P_2^*(\epsilon_1), \ \tilde{S}(\cdot, t) = S(\cdot, t) - S_2^*(\epsilon_1)$ and $\tilde{U}(t) = (\tilde{N}(\cdot, t), \tilde{P}(\cdot, t), \tilde{S}(\cdot, t))$, then dropping the tildes for simplification, system (2.12) can be rewritten into the following abstract form:

$$\frac{dU(t)}{dt} = D(\epsilon)U_{xx} + L(\epsilon_1)U + F(U, \epsilon_1), \tag{3.2}$$

where

$$F(U, \epsilon_1) = (f^{(1)}(N, P, S, \epsilon_1), f^{(2)}(N, P, S, \epsilon_1), f^{(3)}(N, P, S, \epsilon_1))^T - L(\epsilon_1)U, \tag{3.3}$$

with

$$f^{(1)}(N, P, S, \epsilon_1) = r(N + N_2^*(\epsilon_1))\left(1 - \frac{N + N_2^*(\epsilon_1)}{k}\right) - \frac{\beta(N + N_2^*(\epsilon_1))(P + P_2^*(\epsilon_1))}{1 + (\sigma^* + \epsilon_1)(N + N_2^*(\epsilon_1))},$$
$$f^{(2)}(N, P, S, \epsilon_1) = \beta\left(\frac{\gamma(N + N_2^*(\epsilon_1))(P + P_2^*(\epsilon_1))}{1 + (\sigma^* + \epsilon_1)(N + N_2^*(\epsilon_1))} - \rho(P + P_2^*(\epsilon_1))\right),$$
$$f^{(3)}(N, P, S, \epsilon_1) = \xi(N + N_2^*(\epsilon_1)) - \eta(S + S_2^*(\epsilon_1)),$$

and

$$D(\epsilon)U_{xx} = DU_{xx} + G^d(U, \epsilon),$$

with

$$G^d(U, \epsilon) = \begin{pmatrix} 0 \\ -\chi^* P_x S_x \\ 0 \end{pmatrix} + \epsilon_1 D_1 U_{xx} + \epsilon_2 D_2 U_{xx}$$
$$- \epsilon_2 \begin{pmatrix} 0 \\ P_x S_x \\ 0 \end{pmatrix} - \epsilon_1 \epsilon_2 \begin{pmatrix} 0 \\ P_2^{*\prime}(0) S_{xx} \\ 0 \end{pmatrix} + o(\epsilon),$$

where

$$D=\begin{pmatrix}\delta_N & 0 & 0\\ 0 & \delta_P & -\chi^* P_2^*\\ 0 & 0 & \delta_S\end{pmatrix},\quad D_1=\begin{pmatrix}0 & 0 & 0\\ 0 & 0 & -\chi^* P_2^{*\prime}(0)\\ 0 & 0 & 0\end{pmatrix},\quad D_2=\begin{pmatrix}0 & 0 & 0\\ 0 & 0 & -P_2^*\\ 0 & 0 & 0\end{pmatrix},$$

and

$$L(\epsilon_1)U=\begin{pmatrix}a_{11}(\epsilon_1) & a_{12}(\epsilon_1) & 0\\ a_{21}(\epsilon_1) & a_{22}(\epsilon_1) & 0\\ \xi & 0 & -\eta\end{pmatrix}\triangleq AU+\epsilon_1 QU+o(\epsilon_1),$$

where

$$\begin{aligned}a_{11}(\epsilon_1)&=\rho r\left(\frac{1}{\gamma}\left(\sigma^*+\epsilon_1+\frac{1}{k}\right)-\frac{2}{k(\gamma-(\sigma^*+\epsilon_1)\rho)}\right),\ a_{12}=-\frac{\beta\rho}{\gamma},\\ a_{21}(\epsilon_1)&=r\left(\gamma-\rho\left(\sigma^*+\epsilon_1+\frac{1}{k}\right)\right),\ a_{22}(\epsilon_1)=0,\end{aligned}\tag{3.4}$$

and

$$A=\begin{pmatrix}a_{11}(0) & a_{12}(0) & 0\\ a_{21}(0) & a_{22}(0) & 0\\ \xi & 0 & -\eta\end{pmatrix},\quad Q=\begin{pmatrix}a_{11}{}'(0) & 0 & 0\\ a_{21}{}'(0) & 0 & 0\\ 0 & 0 & 0\end{pmatrix}.$$

Noticing that ϵ_1,ϵ_2 are the parameters, we can obtain another form of (3.2) as follows:

$$\frac{dU(t)}{dt}=DU_{xx}+AU+\tilde{F}(U,\epsilon_1,\epsilon_2),\tag{3.5}$$

where

$$\tilde{F}(U,\epsilon_1,\epsilon_2)=F(U,\epsilon_1)+\epsilon_1 QU+G^d(U,\epsilon)+o(\epsilon_1).\tag{3.6}$$

The linearized system of system (2.12) at the origin is

$$\frac{dU}{dt}=DU_{xx}+AU.\tag{3.7}$$

By Theorem 2.5, the operator $D+A$ has two pairs of purely imaginary eigenvalues $\pm i\omega_{n_1},\ \pm i\omega_{n_2}$ $(\omega_{n_1}\neq\omega_{n_2})$ for $n=n_1$ and $n=n_2$ and all other eigenvalues have negative real parts.

Set

$$\mathfrak{B}_n=Span\{[\phi(\cdot),\beta_n^{(j)}]\beta_n^{(j)}|\phi\in X,\ j=1,2,3\},$$

where $\beta_n^{(j)}(x),\ j=1,2,3$ are defined in (2.3).

On $\mathfrak{B}_n$, the linear equation (3.7) is equivalent to the ODE on R^3:

$$\begin{pmatrix}\dot N\\ \dot P\\ \dot S\end{pmatrix}=\begin{pmatrix}-\delta_N\left(\frac{n}{l}\right)^2 & 0 & 0\\ 0 & -\delta_P\left(\frac{n}{l}\right)^2 & \chi^* P_2^*\left(\frac{n}{l}\right)^2\\ 0 & 0 & -\delta_S\left(\frac{n}{l}\right)^2\end{pmatrix}\begin{pmatrix}N\\ P\\ S\end{pmatrix}+A\begin{pmatrix}N\\ P\\ S\end{pmatrix},\tag{3.8}$$

where $(N,P,S)\in R^3$. It is easy to check that (3.8) has the same characteristic equation as the linearized equation (3.7).

Let

$$\mathscr{M}_n=\left(\frac{n}{l}\right)^2 D+A\tag{3.9}$$

be the characteristic matrix of (3.8). Let Λ be the finite set of all eigenvalues of the matrix (3.9) with zero real parts. We have known, when $n=n_1,\ n_2$, $\mathscr{M}_n$ has two pairs of purely imaginary roots $\pm i\omega_{n_1},\pm i\omega_{n_2}$, i.e. $\Lambda=\{i\omega_{n_1},-i\omega_{n_1},i\omega_{n_2},-i\omega_{n_2}\}$. And P is the generalized eigenspace corresponding to Λ. P^* is the dual space of P.

Define the scalar product

$$\langle \psi^T, \phi \rangle = \psi^T \phi, \text{ for } \psi, \phi \in R^3.$$

Denote

$$\Phi_{n_1} = (\phi_1, \phi_2), \ \Phi_{n_2} = (\phi_3, \phi_4),$$
$$\Psi_{n_1} = col(\psi_1^T, \psi_2^T), \Psi_{n_2} = col(\psi_3^T, \psi_4^T).$$

Let $\Phi \doteq (\Phi_{n_1}, \Phi_{n_2}) = (\phi_1, \phi_2, \phi_3, \phi_4)$, $\Psi \doteq diag(\Psi_{n_1}, \Psi_{n_2})$ be the basis of P and P^* associated with the eigenvalues $i\omega_{n_1}$ and $i\omega_{n_2}$ satisfying

$$\mathscr{M}_n \Phi_n = \Phi_n B_n, \ \mathscr{M}_n^T \Psi_n = B_n \Psi_n, \langle \Psi_n, \Phi_n \rangle = I, \ n = n_1, n_2,$$

with $B_{n_1} = diag(i\omega_{n_1}, -i\omega_{n_1})$, $B_{n_2} = diag(i\omega_{n_2}, -i\omega_{n_2})$.

By virtue of $\mathscr{M}_{n_1} \Phi_{n_1} = \Phi_{n_1} B_{n_1}$, $\mathscr{M}_{n_1}^T \Psi_{n_1} = B_{n_1} \Psi_{n_1}$, i.e.

$$\mathscr{M}_{n_1} \phi_1 = i\omega_{n_1} \phi_1, \ \mathscr{M}_{n_1} \phi_2 = -i\omega_{n_1} \phi_2, \ \mathscr{M}_{n_1}^T \psi_1^T = i\omega_{n_1} \psi_1^T, \ \mathscr{M}_{n_1}^T \psi_2^T = -i\omega_{n_1} \psi_2^T,$$

we choose that

$$\phi_1 = \begin{pmatrix} \phi_{11} \\ \phi_{12} \\ \phi_{13} \end{pmatrix} = \begin{pmatrix} 1 \\ \frac{i\omega_{n_1} + \delta_N \left(\frac{n_1}{l}\right)^2 - a_{11}(0)}{a_{12}(0)} \\ \frac{\xi}{i\omega_{n_1} + \delta_S \left(\frac{n_1}{l}\right)^2 + \eta} \end{pmatrix},$$

$$\psi_1 = \begin{pmatrix} \psi_{11} \\ \psi_{12} \\ \psi_{13} \end{pmatrix} = \overline{M_1} \begin{pmatrix} \frac{i\omega_{n_1} + \delta_p \left(\frac{n_1}{l}\right)^2 - a_{22}(0)}{a_{12}(0)} \\ 1 \\ \frac{\chi^* P_2^* \left(\frac{n_1}{l}\right)^2}{i\omega_{n_1} + \delta_S \left(\frac{n_1}{l}\right)^2 + \eta} \end{pmatrix},$$

$$\phi_2 = \overline{\phi_1}, \quad \psi_2 = \overline{\psi_1},$$

with

$$\overline{M_1} = \left(\frac{2i\omega_{n_1} + (\delta_P + \delta_N) \left(\frac{n_1}{l}\right)^2 - a_{11}(0) - a_{22}(0)}{a_{12}(0)} + \frac{\xi \chi^* P_2^* \left(\frac{n_1}{l}\right)^2}{(i\omega_{n_1} + \delta_S \left(\frac{n_1}{l}\right)^2 + \eta)^2} \right)^{-1}.$$

By the same way, in terms of $\mathscr{M}_{n_2} \Phi_{n_2} = \Phi_{n_2} B_{n_2}$, $\mathscr{M}_{n_2}^T \Psi_{n_2} = B_{n_2} \Psi_{n_2}$, i.e.

$$\mathscr{M}_{n_2} \phi_3 = i\omega_{n_2} \phi_3, \ \mathscr{M}_{n_2} \phi_4 = -i\omega_{n_2} \phi_4, \ \mathscr{M}_{n_2}^T \psi_3^T = i\omega_{n_2} \psi_3^T, \ \mathscr{M}_{n_2}^T \psi_4^T = -i\omega_{n_2} \psi_4^T,$$

we choose that

$$\phi_3 = \begin{pmatrix} \phi_{31} \\ \phi_{32} \\ \phi_{33} \end{pmatrix} = \begin{pmatrix} 1 \\ \frac{i\omega_{n_2} + \delta_N \left(\frac{n_2}{l}\right)^2 - a_{11}(0)}{a_{12}(0)} \\ \frac{\xi}{i\omega_{n_2} + \delta_S \left(\frac{n_2}{l}\right)^2 + \eta} \end{pmatrix}, \quad \psi_3 = \begin{pmatrix} \psi_{31} \\ \psi_{32} \\ \psi_{33} \end{pmatrix} = \overline{M_2} \begin{pmatrix} \frac{i\omega_{n_2} + \delta_p \left(\frac{n_2}{l}\right)^2 - a_{22}(0)}{a_{12}(0)} \\ 1 \\ \frac{\chi^* P_2^* \left(\frac{n_2}{l}\right)^2}{i\omega_{n_2} + \delta_S \left(\frac{n_2}{l}\right)^2 + \eta} \end{pmatrix},$$

$$\phi_4 = \overline{\phi_3}, \quad \psi_4 = \overline{\psi_3},$$

with

$$\overline{M_2} = \left(\frac{2i\omega_{n_2} + (\delta_P + \delta_N) \left(\frac{n_2}{l}\right)^2 - a_{11}(0) - a_{22}(0)}{a_{12}(0)} + \frac{\xi \chi^* P_2^* \left(\frac{n_2}{l}\right)^2}{(i\omega_{n_2} + \delta_S \left(\frac{n_2}{l}\right)^2 + \eta)^2} \right)^{-1}.$$

Now, we decompose the Sobolev space X into a center subspace P and its orthocomplement, i.e.

$$X = P \oplus ker\pi,$$

where $\pi : X \to P$ is the projection defined by

$$\pi(\phi) = \Phi_{n_1}\langle \Psi_{n_1}, [\phi(\cdot), \beta_{n_1}]\rangle \cdot \beta_{n_1} + \Phi_{n_2}\langle \Psi_{n_2}, [\phi(\cdot), \beta_{n_2}]\rangle \cdot \beta_{n_2}, \tag{3.10}$$

with

$$\left[\phi(\cdot), \beta_{n_j}\right] = \begin{pmatrix} \left[\phi(\cdot), \beta_{n_j}^{(1)}\right] \\ \left[\phi(\cdot), \beta_{n_j}^{(2)}\right] \end{pmatrix}, \ j = 1, 2.$$

By (3.10), $U = (N, P, S)^T \in X$ can be rewritten as

$$\begin{aligned} U &= \Phi_{n_1}\tilde{z}_{n_1} \cdot \beta_{n_1} + \Phi_{n_2}\tilde{z}_{n_2} \cdot \beta_{n_2} + w \\ &= (z_1\phi_1 + z_2\overline{\phi}_1)r_{n_1}(x) + (z_3\phi_3 + z_4\overline{\phi}_3)r_{n_2}(x) + w \\ &\doteq \Phi z_x + w, \end{aligned} \tag{3.11}$$

where $\tilde{z}_{n_1} = \langle \Psi_{n_1}, [U, \beta_{n_1}]\rangle = (z_1, z_2)$, $\tilde{z}_{n_2} = \langle \Psi_{n_2}, [U, \beta_{n_2}]\rangle = (z_3, z_4)$, and

$$\begin{aligned} z_x &= (z_1 r_{n_1}(x), z_2 r_{n_1}(x), z_3 r_{n_2}(x), z_4 r_{n_2}(x))^T, \\ w &= (w_1, w_2, w_3)^T \in Q \triangleq C^1 \cap Ker\pi = \{\phi \in Ker\pi | \dot{\phi} \in C\}. \end{aligned}$$

For convenience, denote $z \doteq (\tilde{z}_{n_1}, \tilde{z}_{n_2})^T = (z_1, z_2, z_3, z_4)$ and $B = diag(i\omega_{n_1}, -i\omega_{n_1}, i\omega_{n_2}, -i\omega_{n_2})$. Then system (3.5) is decomposed as a system of abstract ODEs on $R^4 \times Ker\pi$:

$$\begin{cases} \dot{z} = Bz + \Psi \begin{pmatrix} [\tilde{F}(\Phi z_x + w, \epsilon), \beta_{n_1}] \\ [\tilde{F}(\Phi z_x + w, \epsilon), \beta_{n_2}] \end{pmatrix}, \\ \dot{w} = L_1 w + (I - \pi)\tilde{F}(\Phi z_x + w, \epsilon), \end{cases} \tag{3.12}$$

where L_1 is the restriction of the linear operator $D + A$ in Q.

3.2 Center Manifold Reduction

Consider the formal Taylor expansion

$$\tilde{F}(U, \epsilon) = \sum_{j \ge 2} \frac{1}{j!}\tilde{F}_j(U, \epsilon), \quad F(U, \epsilon_1) = \sum_{j \ge 2} \frac{1}{j!}F_j(U, \epsilon_1),$$

where $\tilde{F}_j$ is the jth Fr$\acute{e}$chet derivative of $\tilde{F}$. And

$$G^d(U, \epsilon) = \frac{1}{2}G_2^d(U, \epsilon) + \frac{1}{3!}G_3^d(U, \epsilon) + o(\epsilon),$$

where

$$\begin{aligned} G_2^d(U, \epsilon) &= G_2^{d(0,0)}(U) + \epsilon_1 G_2^{d(1,0)}(U) + \epsilon_2 G_2^{d(0,1)}(U), \\ G_3^d(U, \epsilon) &= \epsilon_1 G_3^{d(1,0)}(U) + \epsilon_2 G_3^{d(0,1)}(U) + \epsilon_1\epsilon_2 G_3^{d(1,1)}(U), \end{aligned} \tag{3.13}$$

with

$$G_2^{d(0,0)}(U) = 2\begin{pmatrix} 0 \\ -\chi^* P_x S_x \\ 0 \end{pmatrix}, \quad G_2^{d(1,0)}(U) = 2D_1 U_{xx},$$
$$G_2^{d(0,1)}(U) = 2D_2 U_{xx}, \quad G_3^{d(1,0)}(U) = 0, \tag{3.14}$$
$$G_3^{d(0,1)}(U) = -6\begin{pmatrix} 0 \\ P_x S_x \\ 0 \end{pmatrix}, \quad G_3^{d(1,1)}(U) = -6\begin{pmatrix} 0 \\ P_2^{*\prime}(0) S_{xx} \\ 0 \end{pmatrix}.$$

From (3.6), we have that,

$$\tilde{F}_2(U, \epsilon_1, \epsilon_2) = 2\epsilon_1 QU + G_2^d(U, \epsilon) + F_2(U, \epsilon_1), \tag{3.15}$$

and

$$\tilde{F}_3(U, \epsilon_1, \epsilon_2) = G_3^d(U, \epsilon) + F_3(U, \epsilon_1). \tag{3.16}$$

Then (3.12) can be written as

$$\begin{cases} \dot{z} = Bz + \sum_{j\geq 2} \frac{1}{j!} \tilde{f}_j^1(z, w, \epsilon), \\ \dot{w} = L_1 w + \sum_{j\geq 2} \frac{1}{j!} \tilde{f}_j^2(z, w, \epsilon), \end{cases} \tag{3.17}$$

where

$$\begin{cases} \tilde{f}_j^1(z, w, \epsilon) &= \Psi \begin{pmatrix} [\tilde{F}_j(\Phi z_x + w, \epsilon), \beta_{n_1}] \\ [\tilde{F}_j(\Phi z_x + w, \epsilon), \beta_{n_2}] \end{pmatrix}, \\ \tilde{f}_j^2(z, w, \epsilon) &= (I - \pi)\tilde{F}_j(\Phi z_x + w, \epsilon). \end{cases} \tag{3.18}$$

Let $V_j^6(R^4)$ denote the space of homogeneous polynomials of degree j in 6 variables $z = (z_1, z_2, z_3, z_4)^T$, $\epsilon = (\epsilon_1, \epsilon_2)^T$ with coefficients in R^4 as follows:

$$V_j^6(R^4) = Span\{z_1^{q_1} z_2^{q_2} z_3^{q_3} z_4^{q_4} \epsilon_2^{p_1} \epsilon_1^{p_2} \vartheta_k, \ q_1, q_2, q_3, q_4, p_1, p_2 \in N_0,$$
$$\text{and } q_1 + q_2 + q_3 + q_4 + p_1 + p_2 = j\},$$

where $\vartheta_k (k = 1, 2, 3, 4)$ are unit coordinate vector of R^4.

Define the operator $M_j = (M_j^1, M_j^2), \ j \geq 2$ by

$$M_j^1 : V_j^6(R^4) \to V_j^6(R^4), \ M_j^2 : V_j^6(Q_1) \to V_j^6(Ker\pi),$$
$$(M_j^1 p)(z, \epsilon) = D_z p(z, \epsilon)Bz - Bp(z, \epsilon), \tag{3.19}$$
$$(M_j^2 h)(z, \epsilon) = D_z h(z, \epsilon)Bz - L_1 h(z, \epsilon).$$

It is easy to verify that,

$$M_j^1(z^q \epsilon^p \vartheta_k) = (i\omega_{n_1}(q_1 - q_2) + i\omega_{n_2}(q_3 - q_4) + (-1)^k i\omega_{n_1}) z^q \epsilon^p \vartheta_k, \ k = 1, 2,$$
$$M_j^1(z^q \epsilon^p \vartheta_k) = (i\omega_{n_1}(q_1 - q_2) + i\omega_{n_2}(q_3 - q_4) + (-1)^k i\omega_{n_2}) z^q \epsilon^p \vartheta_k, \ k = 3, 4, \tag{3.20}$$

where $z^q \epsilon^p = z_1^{q_1} z_2^{q_2} z_3^{q_3} z_4^{q_4} \epsilon_2^{p_1} \epsilon_1^{p_2}$.

Then from (3.20), we have that,

$$Ker(M_2^1) = Span\left\{\begin{pmatrix} z_1\epsilon_i \\ 0 \\ 0 \\ 0 \end{pmatrix}, \begin{pmatrix} 0 \\ z_2\epsilon_i \\ 0 \\ 0 \end{pmatrix}, \begin{pmatrix} 0 \\ 0 \\ z_3\epsilon_i \\ 0 \end{pmatrix}, \begin{pmatrix} 0 \\ 0 \\ 0 \\ z_4\epsilon_i \end{pmatrix}\right\}, \ i = 1, 2,$$

and

$$\begin{aligned} Ker(M_3^1) = Span\{&z_1z_3z_4\vartheta_1, z_1\epsilon_i^2\vartheta_1, z_1^2z_2\vartheta_1, z_1\epsilon_2\epsilon_1\vartheta_1,\\ &z_2z_3z_4\vartheta_2, z_2\epsilon_i^2\vartheta_2, z_1z_2^2\vartheta_2, z_2\epsilon_2\epsilon_1\vartheta_2,\\ &z_1z_2z_3\vartheta_3, z_3\epsilon_i^2\vartheta_3, z_3^2z_4\vartheta_3, z_3\epsilon_2\epsilon_1\vartheta_3,\\ &z_1z_2z_4\vartheta_4, z_4\epsilon_i^2\vartheta_4, z_3z_4^2\vartheta_4, z_4\epsilon_2\epsilon_1\vartheta_4, i = 1, 2\}. \end{aligned}$$

Remark 3.1 If $\omega_{n_1} : \omega_{n_2}$ is $1 : 1$, $1 : 2$, $1 : 3$ or $1 : 4$, that is the strong resonance case, the base forms of the space $Ker(M_2^1)$, $Ker(M_3^1)$ will be more complex, which is not considered here.

For autonomous ODEs in the finite dimension space [10], by a recursive transformation of variables

$$(z, w) = (\tilde{z}, \tilde{w}) + \frac{1}{j!}(U_j^1(\tilde{z}, \epsilon), U_j^2(\tilde{z}, \epsilon)),\ \ j \geq 2,$$

where U_j^1 and U_j^2 are homogeneous polynomials of j in $\tilde{z}$ and ϵ, and dropping the tilde, the normal form on the center manifold for (3.17) is

$$\dot{z} = Bz + \frac{1}{2}g_2^1(z, 0, \epsilon) + \frac{1}{3!}g_3^1(z, 0, \epsilon) + o(\epsilon|z|^2), \tag{3.21}$$

where g_2^1 and g_3^1 are the second and third terms in (z, ϵ), defined by

$$g_2^1(z, 0, \epsilon) = Proj_{Ker(M_2^1)}\tilde{f}_2^1(z, 0, \epsilon),\ \ g_3^1(z, 0, \epsilon) = Proj_{Ker(M_3^1)}\bar{f}_3^1(z, 0, 0) + o(\epsilon|z|^2), \tag{3.22}$$

where

$$\begin{aligned} \bar{f}_3^1(z, 0, 0) =& \tilde{f}_3^1(z, 0, 0) + \frac{3}{2}[(D_z\tilde{f}_2^1)(z, 0, 0)U_2^1(z, 0) + (D_w\tilde{f}_2^1)(z, 0, 0)U_2^2(z, 0)\\ &- (D_zU_2^1(z, 0))g_2^1(z, 0, 0)]. \end{aligned} \tag{3.23}$$

3.3 Second Order Terms of the Normal Form

It follows from (3.18) that,

$$\tilde{f}_2^1(z, 0, \epsilon) = \Psi\begin{pmatrix} \left[\tilde{F}_2(\Phi z_x, \epsilon), \beta_{n_1}\right] \\ \left[\tilde{F}_2(\Phi z_x, \epsilon), \beta_{n_2}\right] \end{pmatrix}. \tag{3.24}$$

From (3.11) and (3.14), we have that,

$$\begin{aligned} &\begin{pmatrix} \left[2\epsilon_1 Q(\Phi z_x), \beta_{n_1}\right] \\ \left[2\epsilon_1 Q(\Phi z_x), \beta_{n_2}\right] \end{pmatrix} = \begin{pmatrix} 2\epsilon_1 Q(z_1\phi_1 + z_2\overline{\phi_1}) \\ 2\epsilon_1 Q(z_3\phi_3 + z_4\overline{\phi_3}) \end{pmatrix},\\ &\begin{pmatrix} \left[\epsilon_1 G_2^{d(1,0)}(\Phi z_x), \beta_{n_1}\right] \\ \left[\epsilon_1 G_2^{d(1,0)}(\Phi z_x), \beta_{n_2}\right] \end{pmatrix} = \begin{pmatrix} -2\epsilon_1\left(\frac{n_1}{l}\right)^2 D_1(z_1\phi_1 + z_2\overline{\phi_1}) \\ -2\epsilon_1\left(\frac{n_2}{l}\right)^2 D_1(z_3\phi_3 + z_4\overline{\phi_3}) \end{pmatrix},\\ &\begin{pmatrix} \left[\epsilon_2 G_2^{d(0,1)}(\Phi z_x), \beta_{n_1}\right] \\ \left[\epsilon_2 G_2^{d(0,1)}(\Phi z_x), \beta_{n_2}\right] \end{pmatrix} = \begin{pmatrix} -2\epsilon_2\left(\frac{n_1}{l}\right)^2 D_2(z_1\phi_1 + z_2\overline{\phi_1}) \\ -2\epsilon_2\left(\frac{n_2}{l}\right)^2 D_2(z_3\phi_3 + z_4\overline{\phi_3}) \end{pmatrix}. \end{aligned} \tag{3.25}$$

From (3.3), it is easy to check that for any $\epsilon \in R^2_+$,

$$F_2(\Phi z_x, \epsilon) = F_2(\Phi z_x, 0),$$

which, together with (3.15), (3.22), (3.25) results in

$$\frac{1}{2} g_2^1(z, 0, \epsilon) = \frac{1}{2} Proj_{Ker(M_2^1)} \tilde{f}_2^1(z, 0, \epsilon) = \begin{pmatrix} B_{n_1 1} z_1 \epsilon_1 + B_{n_1 2} z_1 \epsilon_2 \\ \overline{B_{n_1 1}} z_2 \epsilon_1 + \overline{B_{n_1 2}} z_2 \epsilon_2 \\ B_{n_2 1} z_3 \epsilon_1 + B_{n_2 2} z_3 \epsilon_2 \\ \overline{B_{n_2 1}} z_4 \epsilon_1 + \overline{B_{n_2 2}} z_4 \epsilon_2 \end{pmatrix}, \tag{3.26}$$

where

$$B_{n_1 1} = \psi_1^T \left(Q\phi_1 - \left(\frac{n_1}{l}\right)^2 D_1 \phi_1 \right), \quad B_{n_1 2} = -\left(\frac{n_1}{l}\right)^2 \psi_1^T D_2 \phi_1,$$
$$B_{n_2 1} = \psi_3^T \left(Q\phi_3 - \left(\frac{n_2}{l}\right)^2 D_1 \phi_3 \right), \quad B_{n_2 2} = -\left(\frac{n_2}{l}\right)^2 \psi_3^T D_2 \phi_3.$$

3.4 Third Order Terms of the Normal Form

Since $o(|z|\epsilon^2)$ is irrelevant to determine the generic Hopf bifurcation, it is sufficient to compute $g_3^1(z, 0, 0)$ for determining the properties of Hopf bifurcation.

By (3.22), (3.23) and $g_2^1(z, 0, 0) = (0, 0, 0, 0)^T$, we have that,

$$g_3^1(z, 0, 0) = Proj_{Ker(M_3^1)} \bar{f}_3^1(z, 0, 0), \tag{3.27}$$

where

$$\bar{f}_3^1(z, 0, 0) = \tilde{f}_3^1(z, 0, 0) + \frac{3}{2}[(D_z \tilde{f}_2^1)(z, 0, 0)U_2^1(z, 0) + (D_w \tilde{f}_2^1)(z, 0, 0)U_2^2(z, 0)],$$

and

$$U_2^1 = (M_2^1)^{-1} \tilde{f}_2^1(z, 0, 0), \; U_2^2 = (M_2^2)^{-1} \tilde{f}_2^2(z, 0, 0). \tag{3.28}$$

Next we calculate the third order terms $g_3^1(z, 0, 0)$ in three steps.

Step 1. The calculation of $Proj_{Ker(M_3^1)} \tilde{f}_3^1(z, 0, 0)$.

By (3.13) and (3.16), we have that,

$$\tilde{F}_3(\Phi z_x, 0) = F_3(\Phi z_x, 0).$$

Expand $F_3(\Phi z_x, 0)$ in Taylor series described as follows:

$$\tilde{F}_3(\Phi z_x, 0) = F_3(\Phi z_x, 0) = \sum_{q_1+q_2+q_3+q_4=3} F_{q_1 q_2 q_3 q_4} r_{n_1}^{q_1+q_2}(x) r_{n_2}^{q_3+q_4}(x) z_1^{q_1} z_2^{q_2} z_3^{q_3} z_4^{q_4},$$

where $F_{q_1 q_2 q_3 q_4} = (F^{(1)}_{q_1 q_2 q_3 q_4}, F^{(2)}_{q_1 q_2 q_3 q_4}, F^{(3)}_{q_1 q_2 q_3 q_4})^T$. Hence, from (3.18), we have that,

$$\tilde{f}_3^1(z, 0, 0) = \Psi \begin{pmatrix} \left[\tilde{F}_3(\Phi z_x, 0), \beta_{n_1}\right] \\ \left[\tilde{F}_3(\Phi z_x, 0), \beta_{n_2}\right] \end{pmatrix} = \Psi \begin{pmatrix} \left[F_3(\Phi z_x, 0), \beta_{n_1}\right] \\ \left[F_3(\Phi z_x, 0), \beta_{n_2}\right] \end{pmatrix}$$
$$= \Psi \begin{pmatrix} \sum_{q_1+q_2+q_3+q_4=3} F_{q_1 q_2 q_3 q_4} \int_0^{l\pi} r_{n_1}^{q_1+q_2+1}(x) r_{n_2}^{q_3+q_4}(x) dx z_1^{q_1} z_2^{q_2} z_3^{q_3} z_4^{q_4} \\ \sum_{q_1+q_2+q_3+q_4=3} F_{q_1 q_2 q_3 q_4} \int_0^{l\pi} r_{n_1}^{q_1+q_2}(x) r_{n_2}^{q_3+q_4+1}(x) dx z_1^{q_1} z_2^{q_2} z_3^{q_3} z_4^{q_4} \end{pmatrix}.$$

Therefore,

$$\frac{1}{3!}Proj_{Ker(M_3^1)}\tilde{f}_3^1(z,0,0)=\begin{pmatrix} C_{2100}z_1^2z_2+C_{1011}z_1z_3z_4\\ \overline{C_{2100}}z_1z_2^2+\overline{C_{1011}}z_2z_3z_4\\ C_{0021}z_3^2z_4+C_{1110}z_1z_2z_3\\ \overline{C_{0021}}z_3z_4^2+\overline{C_{1110}}z_1z_2z_4 \end{pmatrix}, \tag{3.29}$$

where, combining with the fact $\int_0^{l\pi} r_{n_1}^2(x)r_{n_2}^2(x)dx=\frac{1}{l\pi}$,

$$C_{2100}=\begin{cases}\frac{1}{6l\pi}\psi_1^T F_{2100},\ n_1=0,\\ \frac{1}{4l\pi}\psi_1^T F_{2100},\ n_1\neq 0,\end{cases}\qquad C_{1011}=\frac{1}{6l\pi}\psi_1^T F_{1011},$$
$$C_{0021}=\frac{1}{4l\pi}\psi_3^T F_{0021},\qquad C_{1110}=\frac{1}{6l\pi}\psi_3^T F_{1110}.$$

Step 2. The calculation of $Proj_{Ker(M_3^1)}(D_z\tilde{f}_2^1)(z,0,0)U_2^1(z,0)$.

It follows from (3.13),(3.15) that

$$\tilde{F}_2(\Phi z_x,0)=G_2^d(\Phi z_x,0)+F_2(\Phi z_x,0)=G_2^{d(0,0)}(\Phi z_x)+F_2(\Phi z_x,0). \tag{3.30}$$

Since for all $\epsilon\in R^2$, $F(0,\epsilon)=DF(0,\epsilon)U=(0,0,0)^T$. Then we have that,

$$\begin{aligned}&F_2(\Phi z_x+w,\epsilon)=F_2(\Phi z_x+w,0)\\ &=\sum_{q_1+q_2+q_3+q_4=2}F_{q_1q_2q_3q_4}r_{n_1}^{q_1+q_2}(x)r_{n_2}^{q_3+q_4}(x)z_1^{q_1}z_2^{q_2}z_3^{q_3}z_4^{q_4}+S_2(\Phi z_x+w,0)+o(|w|^2),\end{aligned} \tag{3.31}$$

where $S_2(\Phi z_x+w,0)$ is the cross term of Φz_x and w.

Besides, denote $G_2^{d(0,0)}(\Phi z_x)=(0,G_2^{d(0,0)(2)}(\Phi z_x),0)^T$ for convenience. From (3.14), we have that,

$$\begin{aligned}&G_2^{d(0,0)(2)}(\Phi z_x)\\ &\quad=-\frac{4}{l\pi}\chi^*\Bigg\{\left(\frac{n_1}{l}\right)^2(\phi_{12}\phi_{13}z_1^2+2Re(\phi_{12}\overline{\phi_{13}})z_1z_2+\overline{\phi_{12}\phi_{13}}z_2^2)\left(\sin\frac{n_1x}{l}\right)^2\\ &\quad+\frac{n_1n_2}{l^2}((\phi_{12}\phi_{33}+\phi_{13}\phi_{32})z_1z_3+(\phi_{12}\overline{\phi_{33}}+\phi_{13}\overline{\phi_{32}})z_1z_4\\ &\quad+(\overline{\phi_{12}}\phi_{33}+\overline{\phi_{13}}\phi_{32})z_2z_3+(\overline{\phi_{12}\phi_{33}}+\overline{\phi_{13}\phi_{32}})z_2z_4)\sin\frac{n_1x}{l}\sin\frac{n_2x}{l}\\ &\quad+\left(\frac{n_2}{l}\right)^2(\phi_{32}\phi_{33}z_3^2+2Re(\phi_{32}\overline{\phi_{33}})z_3z_4+\overline{\phi_{32}\phi_{33}}z_4^2)\left(\sin\frac{n_2x}{l}\right)^2\Bigg\}.\end{aligned} \tag{3.32}$$

Noticing that,

$$
\begin{aligned}
&\int_0^{l\pi} r_m^2(x) r_n(x) dx = \begin{cases} \frac{1}{\sqrt{l\pi}}, & m \neq 0,\ n = 0, \\ \frac{1}{\sqrt{2l\pi}}, & 2m = n \neq 0, \\ 0, & \text{otherwise}, \end{cases} \\
&\int_0^{l\pi} \left(\sin \frac{mx}{l}\right)^2 r_n(x) dx = \begin{cases} \frac{\sqrt{l\pi}}{2}, & m \neq 0,\ n = 0, \\ -\frac{\sqrt{2l\pi}}{4}, & 2m = n \neq 0, \\ 0, & \text{otherwise}, \end{cases} \\
&\int_0^{l\pi} \sin \frac{mx}{l} \sin \frac{nx}{l} r_k(x) dx = \begin{cases} \frac{\sqrt{2l\pi}}{4}, & k = n - m,\ m \neq 0, \\ -\frac{\sqrt{2l\pi}}{4}, & k = n + m, \\ 0, & \text{otherwise}, \end{cases} \\
&\int_0^{l\pi} r_m(x) r_n(x) r_k(x) dx = \begin{cases} \frac{1}{\sqrt{2l\pi}}, & k = m + n, \ \text{or}\ k = n - m. \\ 0, & \text{otherwise}. \end{cases}
\end{aligned}
\tag{3.33}
$$

by (3.24), (3.30), (3.33), direct calculation results in

$$
\tilde{f}_2^1(z, 0, 0) = \Psi \begin{pmatrix} \left[\tilde{F}_2(\Phi z_x, 0), \beta_{n_1}\right] \\ \left[\tilde{F}_2(\Phi z_x, 0), \beta_{n_2}\right] \end{pmatrix}
$$

$$
= \begin{cases} \frac{1}{\sqrt{l\pi}} \Psi \begin{pmatrix} F_{2000} z_1^2 + \overline{F_{2000}} z_2^2 + (F_{0020} - E_1) z_3^2 + (\overline{F_{0020}} - \overline{E_1}) z_4^2 \\ +(F_{0011} - E_2) z_3 z_4 + F_{1100} z_1 z_2 \\ F_{1010} z_1 z_3 + F_{1001} z_1 z_4 + F_{0110} z_2 z_3 + F_{0101} z_2 z_4 \end{pmatrix}, & n_1 = 0,\ n_2 \neq 0, \\ (0, 0, 0, 0)^T, & n_2 \neq 2n_1, \\ \frac{1}{\sqrt{2l\pi}} \Psi \begin{pmatrix} (F_{1010} - E_3) z_1 z_3 + (F_{1001} - E_4) z_1 z_4 + (F_{0110} - \overline{E_4}) z_2 z_3 \\ +(F_{0101} - \overline{E_3}) z_2 z_4 \\ (F_{2000} + E_5) z_1^2 + (\overline{F_{2000}} + \overline{E_5}) z_2^2 + (F_{1100} + \overline{E_6}) z_1 z_2 \end{pmatrix}, & n_2 = 2n_1, \end{cases}
$$

where

$$
\begin{aligned}
&E_1 = \left(0, 2\chi^* \phi_{32}\phi_{33} \left(\frac{n_2}{l}\right)^2, 0\right)^T,\ E_2 = \left(0, 4\chi^* Re(\phi_{32}\overline{\phi_{33}}) \left(\frac{n_2}{l}\right)^2, 0\right)^T, \\
&E_3 = \left(0, 2\chi^* (\phi_{12}\phi_{33} + \phi_{13}\phi_{32}) \frac{n_1 n_2}{l^2}, 0\right)^T,\ E_4 = \left(0, 2\chi^* (\phi_{12}\overline{\phi_{33}} + \phi_{13}\overline{\phi_{32}}) \frac{n_1 n_2}{l^2}, 0\right)^T, \\
&E_5 = \left(0, 2\chi^* \phi_{12}\phi_{13} \left(\frac{n_1}{l}\right)^2, 0\right)^T,\ E_6 = \left(0, 4\chi^* Re(\phi_{12}\overline{\phi_{13}}) \left(\frac{n_1}{l}\right)^2, 0\right)^T.
\end{aligned}
\tag{3.34}
$$

Thus, for $n_2 \neq 2n_1,\ n_1 \neq 0,\ U_2^1(z, 0) = (0, 0, 0, 0)^T$.

For $n_1 = 0, n_2 \neq 0$, we can compute that $U_2^1(z,0) = (U_2^{1(1)}, U_2^{1(2)}, U_2^{1(3)}, U_2^{1(4)})^T$ from $U_2^1 = (M_2^1)^{-1}\tilde{f}_2^1(z,0,0)$ as follows:

$$
\begin{aligned}
U_2^{1(1)} &= \frac{1}{\sqrt{l\pi}}\psi_1^T\left(\frac{1}{i\omega_{n_1}}F_{2000}z_1^2 - \frac{1}{3i\omega_{n_1}}\overline{F_{2000}}z_2^2 + \frac{1}{2i\omega_{n_2} - i\omega_{n_1}}(F_{0020} - E_1)z_3^2\right.\\
&\quad\left. -\frac{1}{2i\omega_{n_2} + i\omega_{n_1}}(\overline{F_{0020}} - \overline{E_1})z_4^2 - \frac{1}{i\omega_{n_1}}F_{1100}z_1z_2 - \frac{1}{i\omega_{n_1}}(F_{0011} - E_2)z_3z_4\right),\\
U_2^{1(2)} &= \frac{1}{\sqrt{l\pi}}\overline{\psi_1}^T\left(\frac{1}{3i\omega_{n_1}}F_{2000}z_1^2 - \frac{1}{i\omega_{n_1}}\overline{F_{2000}}z_2^2 + \frac{1}{2i\omega_{n_2} + i\omega_{n_1}}(F_{0020} - E_1)z_3^2\right.\\
&\quad\left. -\frac{1}{2i\omega_{n_2} - i\omega_{n_1}}(\overline{F_{0020}} - \overline{E_1})z_4^2 + \frac{1}{i\omega_{n_1}}F_{1100}z_1z_2 + \frac{1}{i\omega_{n_1}}(F_{0011} - E_2)z_3z_4\right),\\
U_2^{1(3)} &= \frac{1}{\sqrt{l\pi}}\psi_3^T\left(\frac{F_{1010}}{i\omega_{n_1}}z_1z_3 - \frac{F_{1001}}{2i\omega_{n_2} - i\omega_{n_1}}z_1z_4 - \frac{F_{0110}}{i\omega_{n_1}}z_2z_3 - \frac{F_{0101}}{2i\omega_{n_2} + i\omega_{n_1}}z_2z_4\right),\\
U_2^{1(4)} &= \frac{1}{\sqrt{l\pi}}\overline{\psi_3}^T\left(\frac{F_{1010}}{i\omega_{n_1} + 2i\omega_{n_2}}z_1z_3 + \frac{F_{1001}}{i\omega_{n_1}}z_1z_4 - \frac{F_{0110}}{i\omega_{n_1} - 2i\omega_{n_2}}z_2z_3 - \frac{F_{0101}}{i\omega_{n_1}}z_2z_4\right).
\end{aligned}
$$

For $2n_1 = n_2 \neq 0$, $U_2^1(z,0) = (U_2^{1(1)}, U_2^{1(2)}, U_2^{1(3)}, U_2^{1(4)})$ denoted by

$$
\begin{aligned}
U_2^{1(1)} &= \frac{1}{\sqrt{2l\pi}}\psi_1^T\left(\frac{1}{i\omega_{n_2}}(F_{1010} - E_3)z_1z_3 - \frac{1}{i\omega_{n_2}}(F_{1001} - E_4)z_1z_4\right.\\
&\quad\left. +\frac{1}{i\omega_{n_2} - 2i\omega_{n_1}}(F_{0110} - \overline{E_4})z_2z_3 - \frac{1}{i\omega_{n_2} + 2i\omega_{n_1}}(F_{0101} - \overline{E_3})z_2z_4\right),\\
U_2^{1(2)} &= \frac{1}{\sqrt{2l\pi}}\overline{\psi_1}^T\left(\frac{1}{2i\omega_{n_1} + i\omega_{n_2}}(F_{1010} - E_3)z_1z_3 + \frac{1}{2i\omega_{n_1} - i\omega_{n_2}}(F_{1001} - E_4)z_1z_4\right.\\
&\quad\left. +\frac{1}{i\omega_{n_2}}(F_{0110} - \overline{E_4})z_2z_3 - \frac{1}{i\omega_{n_2}}(F_{0101} - \overline{E_3})z_2z_4\right),\\
U_2^{1(3)} &= \frac{1}{\sqrt{2l\pi}}\psi_3^T\left(\frac{F_{2000} + E_5}{2i\omega_{n_1} - i\omega_{n_2}}z_1^2 - \frac{\overline{F_{2000}} + \overline{E_5}}{2i\omega_{n_1} + i\omega_{n_2}}z_2^2 - \frac{F_{1100} + \overline{E_6}}{i\omega_{n_2}}z_1z_2\right),\\
U_2^{1(4)} &= \frac{1}{\sqrt{2l\pi}}\overline{\psi_3}^T\left(\frac{F_{2000} + E_5}{2i\omega_{n_1} + i\omega_{n_2}}z_1^2 - \frac{\overline{F_{2000}} + \overline{E_5}}{2i\omega_{n_1} - i\omega_{n_2}}z_2^2 + \frac{F_{1100} + \overline{E_6}}{i\omega_{n_2}}z_1z_2\right).
\end{aligned}
$$

Thus,

$$
\frac{1}{3!}Proj_{Ker(M_3^1)}[(D_z\tilde{f}_2^1)U_2^1](z,0,0) = \begin{pmatrix} D_{2100}z_1^2z_2 + D_{1011}z_1z_3z_4 \\ \overline{D_{2100}}z_1z_2^2 + \overline{D_{1011}}z_2z_3z_4 \\ D_{0021}z_3^2z_4 + D_{1110}z_1z_2z_3 \\ \overline{D_{0021}}z_3z_4^2 + \overline{D_{1110}}z_1z_2z_4 \end{pmatrix}, \tag{3.35}
$$

where for $n_2 \neq 2n_1,\ n_1 \neq 0$, $D_{2100} = D_{1011} = D_{0021} = D_{1110} = 0$. And for $n_1 = 0$, $n_2 \neq 0$,

$$\begin{aligned}
D_{2100} =& \frac{1}{6l\pi i\omega_{n_1}}\left(-(\psi_1^T F_{2000})(\psi_1^T F_{1100}) + \frac{2}{3}|\psi_1^T F_{2000}|^2 + |\psi_1^T F_{1100}|^2\right),\\
D_{1011} =& \frac{1}{6l\pi}\left(-\frac{2}{i\omega_{n_1}}(\psi_1^T F_{2000})(\psi_1^T(F_{0011}-E_2)) + \frac{1}{i\omega_{n_1}}(\psi_1^T F_{1100})(\overline{\psi_1}^T(F_{0011}-E_2))\right.\\
&-\frac{2}{2i\omega_{n_2}-i\omega_{n_1}}(\psi_1^T(F_{0020}-E_1))(\psi_3^T F_{1001}) + \frac{1}{i\omega_{n_1}}(\psi_1^T(F_{0011}-E_2))(\psi_3^T F_{1010})\\
&\left.+\frac{2}{2i\omega_{n_2}+i\omega_{n_1}}(\psi_1^T(\overline{F_{0020}}-\overline{E_1}))(\overline{\psi_3}^T F_{1010}) + \frac{1}{i\omega_{n_1}}(\psi_1^T(F_{0011}-E_2))(\overline{\psi_3}^T F_{1001})\right),\\
D_{0021} =& \frac{1}{6l\pi}\left(-\frac{1}{i\omega_{n_1}}(\psi_3^T F_{1010})(\psi_1^T(F_{0011}-E_2)) + \frac{1}{2i\omega_{n_2}-i\omega_{n_1}}(\psi_3^T F_{1001})(\psi_1^T(F_{0020}-E_1))\right.\\
&\left.+\frac{1}{i\omega_{n_1}}(\psi_3^T F_{0110})(\overline{\psi_1}^T(F_{0011}-E_2)) + \frac{1}{2i\omega_{n_2}+i\omega_{n_1}}(\psi_3^T F_{0101})(\overline{\psi_1}^T(F_{0020}-E_1))\right),\\
D_{1110} =& \frac{1}{6l\pi}\left(\frac{1}{i\omega_{n_1}}(\psi_3^T F_{0110})(\overline{\psi_1}^T F_{1100}) - \frac{1}{i\omega_{n_1}}(\psi_3^T F_{1010})(\psi_1^T F_{1100}) - \frac{1}{i\omega_{n_1}}(\psi_3^T F_{1010})(\psi_3^T F_{0110})\right.\\
&\left.+\frac{1}{i\omega_{n_1}}(\psi_3^T F_{0110})(\psi_3^T F_{1010}) + \frac{|\psi_3^T F_{1001}|^2}{2i\omega_{n_2}-i\omega_{n_1}} + \frac{|\psi_3^T F_{0101}|^2}{i\omega_{n_1}+2i\omega_{n_2}}\right).
\end{aligned}$$

For $2n_1 = n_2 \neq 0$,

$$\begin{aligned}
D_{2100} =& \frac{1}{12l\pi}\left(-\frac{(\psi_1^T(F_{1010}-E_3))(\psi_3^T(F_{1100}+\overline{E_6}))}{i\omega_{n_2}} + \frac{(\psi_1^T(F_{0110}-\overline{E_4})(\psi_3^T(F_{2000}+E_5))}{2i\omega_{n_1}-i\omega_{n_2}}\right.\\
&\left.+\frac{(\psi_1^T(F_{1001}-E_4))(\overline{\psi_3}^T(F_{1100}+\overline{E_6}))}{i\omega_{n_2}} + \frac{(\psi_1^T(F_{0101}-\overline{E_3}))(\overline{\psi_3}^T(F_{2000}+E_5))}{2i\omega_{n_1}+i\omega_{n_2}}\right),\\
D_{1011} =& \frac{1}{12l\pi}\left(-\frac{(\psi_1^T(F_{1010}-E_3))(\psi_1^T(F_{1001}-E_4))}{i\omega_{n_2}} + \frac{(\psi_1^T(F_{1001}-E_4))(\psi_1^T(F_{1010}-E_3))}{i\omega_{n_2}}\right.\\
&\left.+\frac{1}{2i\omega_{n_1}-i\omega_{n_2}}|\psi_1^T(F_{0110}-\overline{E_4})|^2 + \frac{1}{2i\omega_{n_1}+i\omega_{n_2}}|\psi_1^T(F_{0101}-\overline{E_3})|^2\right),\\
D_{0021} =& 0,\\
D_{1110} =& \frac{1}{12l\pi}\left(\frac{2\psi_3^T(F_{2000}+E_5)(\psi_1^T(F_{0110}-\overline{E_4})}{i\omega_{n_2}-2i\omega_{n_1}} + \frac{(\psi_3^T(F_{1100}+\overline{E_6})(\psi_1^T(F_{1010}-E_3))}{i\omega_{n_2}}\right.\\
&\left.+\frac{2\psi_3^T(\overline{F_{2000}}+\overline{E_5})(\overline{\psi_1}^T(F_{1010}-E_3))}{2i\omega_{n_1}+i\omega_{n_2}} + \frac{(\psi_3^T(F_{1100}+\overline{E_6})(\overline{\psi_1}^T(F_{0110}-\overline{E_4}))}{i\omega_{n_2}}\right).
\end{aligned}$$

Step 3. The calculation of $Proj_{Ker(M_3^1)}(D_w\tilde{f_2^1})(z,0,0)U_2^2(z,0)$.

By (3.13), (3.14), (3.15) and (3.18), we have that,

$$(D_w\tilde{f_2^1})(z,0,0)U_2^2(z,0) = \Psi\begin{pmatrix}\left[D_w\tilde{F}_2(\Phi z_x+w,0)|_{w=0}U_2^2(z,0),\beta_{n_1}\right]\\ \left[(D_w\tilde{F}_2(\Phi z_x+w,0)|_{w=0}U_2^2(z,0),\beta_{n_2}\right]\end{pmatrix}, \tag{3.36}$$

where

$$\tilde{F}_2(\Phi z_x+w,0) = G_2^{d(0,0)}(\Phi z_x+w) + F_2(\Phi z_x+w,0). \tag{3.37}$$

Direct computation shows that

$$D_w G_2^{d(0,0)}(\Phi z_x + w)|_{w=0} U_2^2(z,0) = 0, \tag{3.38}$$

since $G_2^{d(0,0)}(\Phi z_x + w)$ is independent on w.

From (3.31),

$$\begin{aligned} F_2(\Phi z_x + w, 0) &= S_2(\Phi z_x + w, 0) + O(z^2, w^2) \\ &= \sum_{j=1}^{3}\left(\sum_{k=1}^{2} S_{jk} w_j z_k r_{n_1}(x) + \sum_{k=3}^{4} S_{jk} w_j z_k r_{n_2}(x)\right) + O(z^2, w^2), \end{aligned}$$

where $S_{jk} = 2\frac{\partial^2 F_2(\Phi z_x + w, 0)}{\partial w_j \partial z_k}|_{z_k=0,\ w=0}$, $(j = 1, 2, 3,\ k = 1, 2, 3, 4)$, which induces that

$$D_w F_2(\Phi z_x + w, 0)|_{w=0} w = \left(\sum_{k=1}^{2}(S_{1k}\ S_{2k}\ S_{3k}) z_k r_{n_1}(x) + \sum_{k=3}^{4}(S_{1k}\ S_{2k}\ S_{3k}) z_k r_{n_2}(x)\right) w. \tag{3.39}$$

Let

$$U_2^2(z,0) \doteq h(z) = \sum_{n\geq 0} h_n(z) r_n(x), \tag{3.40}$$

with

$$h_n \doteq h_n(z) = \begin{pmatrix} h_n^{(1)}(z) \\ h_n^{(2)}(z) \\ h_n^{(3)}(z) \end{pmatrix} = \sum_{q_1+q_2+q_3+q_4=2} \begin{pmatrix} h^{(1)}_{nq_1q_2q_3q_4} \\ h^{(2)}_{nq_1q_2q_3q_4} \\ h^{(3)}_{nq_1q_2q_3q_4} \end{pmatrix} z_1^{q_1} z_2^{q_2} z_3^{q_3} z_4^{q_4}.$$

According to (3.36)–(3.40), we have that,

$$\begin{aligned} (D_w \tilde{f}_2^1)(z,0,0) U_2^2(z,0) &= \Psi\begin{pmatrix} \left[D_w F_2(\Phi z_x + w, 0)|_{w=0} \sum_{n\geq 0} h_n(z) r_n(x), \beta_{n_1}\right] \\ \left[D_w F_2(\Phi z_x + w, 0)|_{w=0} \sum_{n\geq 0} h_n(z) r_n(x), \beta_{n_2}\right] \end{pmatrix} \\ &= \Psi\begin{pmatrix} [\sum_{n\geq 0}(\sum_{k=1}^{2}(S_{1k}\ S_{2k}\ S_{3k}) h_n(z) z_k r_n(x) r_{n_1}(x) \\ + \sum_{k=3}^{4}(S_{1k}\ S_{2k}\ S_{3k}) h_n(z) z_k r_n(x) r_{n_2}(x), \beta_{n_1}] \\ [\sum_{n\geq 0}(\sum_{k=1}^{2}(S_{1k}\ S_{2k}\ S_{3k}) h_n(z) z_k r_n(x) r_{n_1}(x) \\ + \sum_{k=3}^{4}(S_{1k}\ S_{2k}\ S_{3k}) h_n(z) z_k r_n(x) r_{n_2}(x), \beta_{n_2}] \end{pmatrix} \\ &= \Psi\begin{pmatrix} \sum_{n\geq 0}(b_{nn_1n_1}\sum_{k=1}^{2}(S_{1k}\ S_{2k}\ S_{3k}) h_n z_k + b_{nn_1n_2}\sum_{k=3}^{4}(S_{1k}\ S_{2k}\ S_{3k}) h_n z_k) \\ \sum_{n\geq 0}(b_{nn_1n_2}\sum_{k=1}^{2}(S_{1k}\ S_{2k}\ S_{3k}) h_n z_k + b_{nn_2n_2}\sum_{k=3}^{4}(S_{1k}\ S_{2k}\ S_{3k}) h_n z_k) \end{pmatrix}, \end{aligned}$$

where $n = 0, 1, 2, \ldots$ and

$$b_{nn_1n_1} = \int_0^{l\pi} r_n(x) r_{n_1}^2(x) dx = \begin{cases} \frac{1}{\sqrt{l\pi}}, & n = 0, \\ \frac{1}{\sqrt{2l\pi}}, & n = 2n_1 \neq 0, \\ 0, & otherwise. \end{cases}$$

$$b_{nn_1n_2} = \int_0^{l\pi} r_n(x) r_{n_1}(x) r_{n_2}(x) dx = \begin{cases} \frac{1}{\sqrt{l\pi}}, & n = n_2 \neq 0, n_1 = 0, \\ \frac{1}{\sqrt{2l\pi}}, & 0 < n_1 < n_2,\ n = n_2 + n_1 \text{ or } n = n_2 - n_1, \\ 0, & otherwise. \end{cases}$$

Thus, for $n_1 = 0, n_2 \neq 0$,

$$(D_w \tilde{f_2^1})(z, 0, 0) U_2^2(z, 0) = \Psi \begin{pmatrix} \frac{1}{\sqrt{l\pi}} \left(\sum_{k=1}^2 (S_{1k}\ S_{2k}\ S_{3k}) h_0 z_k + \sum_{k=3}^4 (S_{1k}\ S_{2k}\ S_{3k}) h_{n_2} z_k \right) \\ \frac{1}{\sqrt{l\pi}} \left(\sum_{k=1}^2 (S_{1k}\ S_{2k}\ S_{3k}) h_{n_2} z_k + \sum_{k=3}^4 (S_{1k}\ S_{2k}\ S_{3k}) h_0 z_k \right) \\ + \frac{1}{\sqrt{2l\pi}} \sum_{k=3}^4 (S_{1k}\ S_{2k}\ S_{3k}) h_{(2n_2)} z_k \end{pmatrix}.$$

For $0 < n_1 \leq n_2$,

$$\begin{aligned} &(D_w \tilde{f_2^1})(z, 0, 0) U_2^2(z, 0) \\ &= \Psi \begin{pmatrix} \frac{1}{\sqrt{2l\pi}} \left(\sum_{k=1}^2 (S_{1k}\ S_{2k}\ S_{3k}) h_{2n_1} z_k + \sum_{k=3}^4 (S_{1k}\ S_{2k}\ S_{3k}) h_{n_1+n_2} z_k \right) \\ + \frac{1}{\sqrt{l\pi}} \sum_{k=1}^2 (S_{1k}\ S_{2k}\ S_{3k}) h_0 z_k + \delta_{n_1n_2} \sum_{k=3}^4 (S_{1k}\ S_{2k}\ S_{3k}) h_{n_2-n_1} z_k \\ \frac{1}{\sqrt{2l\pi}} \left(\sum_{k=1}^2 (S_{1k}\ S_{2k}\ S_{3k}) h_{n_1+n_2} z_k + \sum_{k=3}^4 (S_{1k}\ S_{2k}\ S_{3k}) h_{2n_2} z_k \right) \\ + \frac{1}{\sqrt{l\pi}} \sum_{k=3}^4 (S_{1k}\ S_{2k}\ S_{3k}) h_0 z_k + \delta_{n_1n_2} \sum_{k=1}^2 (S_{1k}\ S_{2k}\ S_{3k}) h_{n_2-n_1} z_k \end{pmatrix}, \end{aligned}$$

where $\delta_{n_1n_2} = \begin{cases} \frac{1}{\sqrt{2l\pi}}, & n_1 < n_2 \\ \frac{1}{\sqrt{l\pi}}, & n_1 = n_2 \end{cases}$. Then,

$$\frac{1}{3!} Proj_{Ker(M_3^1)} (D_w \tilde{f_2^1})(z, 0, 0) U_2^2(z, 0) = \begin{pmatrix} E_{2100} z_1^2 z_2 + E_{1011} z_1 z_3 z_4 \\ \overline{E_{2100}} z_1 z_2^2 + \overline{E_{1011}} z_2 z_3 z_4 \\ E_{0021} z_3^2 z_4 + E_{1110} z_1 z_2 z_3 \\ \overline{E_{0021}} z_3 z_4^2 + \overline{E_{1110}} z_1 z_2 z_4 \end{pmatrix}, \tag{3.41}$$

where for $n_1 = 0,\ n_2 \neq 0$,

$$E_{2100} = \frac{1}{6\sqrt{l\pi}}\psi_1^T((S_{11}\ S_{21}\ S_{31})h_{01100} + (S_{12}\ S_{22}\ S_{32})h_{02000}),$$

$$E_{1011} = \frac{1}{6\sqrt{l\pi}}\psi_1^T((S_{11}\ S_{21}\ S_{31})h_{00011} + (S_{13}\ S_{23}\ S_{33})h_{n_2 1001} + (S_{14}\ S_{24}\ S_{34})h_{n_2 1010}),$$

$$E_{0021} = \frac{1}{6}\psi_3^T\left(\frac{1}{\sqrt{l\pi}}((S_{13}\ S_{23}\ S_{33})h_{00011} + (S_{14}\ S_{24}\ S_{34})h_{00020}) + \frac{1}{\sqrt{2l\pi}}((S_{13}\ S_{23}\ S_{33})h_{(2n_2)0011} + (S_{14}\ S_{24}\ S_{34})h_{(2n_2)0020})\right),$$

$$E_{1110} = \frac{1}{6}\psi_3^T\left(\frac{1}{\sqrt{l\pi}}((S_{11}\ S_{21}\ S_{31})h_{n_2 0110} + (S_{12}\ S_{22}\ S_{32})h_{n_2 1010} + (S_{13}\ S_{23}\ S_{33})h_{01100}) + \frac{1}{\sqrt{2l\pi}}(S_{13}\ S_{23}\ S_{33})h_{(2n_2)1100}\right),$$

and for $0 < n_1 \leq n_2$,

$$E_{2100} = \frac{1}{6}\psi_1^T\left(\frac{1}{\sqrt{l\pi}}((S_{11}\ S_{21}\ S_{31})h_{01100} + (S_{12}\ S_{22}\ S_{32})h_{02000}) + \frac{1}{\sqrt{2l\pi}}((S_{11}\ S_{21}\ S_{31})h_{(2n_1)1100} + (S_{12}\ S_{22}\ S_{32})h_{(2n_1)2000})\right),$$

$$E_{1011} = \frac{1}{6}\psi_1^T\left(\frac{1}{\sqrt{2l\pi}}\big((S_{11}\ S_{21}\ S_{31})h_{(2n_1)0011} + (S_{13}\ S_{23}\ S_{33})h_{(n_1+n_2)1001} + (S_{14}\ S_{24}\ S_{34})h_{(n_1+n_2)1010}\big) + \frac{1}{\sqrt{l\pi}}(S_{11}\ S_{21}\ S_{31})h_{00011} + \delta_{n_1 n_2}((S_{13}\ S_{23}\ S_{33})h_{(n_2-n_1)1001} + (S_{14}\ S_{24}\ S_{34})h_{(n_2-n_1)1010})\right),$$

$$E_{0021} = \frac{1}{6}\psi_3^T\left(\frac{1}{\sqrt{2l\pi}}((S_{13}\ S_{23}\ S_{33})h_{(2n_2)0011} + (S_{14}\ S_{24}\ S_{34})h_{(2n_2)0020}) + \frac{1}{\sqrt{l\pi}}((S_{13}\ S_{23}\ S_{33})h_{00011} + (S_{14}\ S_{24}\ S_{34})h_{00020})\right),$$

$$E_{1110} = \frac{1}{6}\psi_3^T\left(\frac{1}{\sqrt{2l\pi}}\big((S_{11}\ S_{21}\ S_{31})h_{(n_1+n_2)0110} + (S_{12}\ S_{22}\ S_{32})h_{(n_1+n_2)1010} + (S_{13}\ S_{23}\ S_{33})h_{(2n_2)1100}\big) + \frac{1}{\sqrt{l\pi}}(S_{13}\ S_{23}\ S_{33})h_{01100} + \delta_{n_1 n_2}(S_{11}\ S_{21}\ S_{31})h_{(n_2-n_1)0110} + (S_{12}\ S_{22}\ S_{32})h_{(n_2-n_1)1010}\right).$$

Obviously, we still need to compute $h_{n1100},\ h_{n2000},\ h_{n0011},\ h_{n1001},\ h_{n1010},\ h_{n0020},\ h_{n0110}$.

By (3.19), we have that,

$$(M_2^2)(h_n(z)r_n(x)) = (D_z)(h_n(z)r_n(x))Bz - L_1(h_n(z)r_n(x)),$$

which, combining (3.1), (3.9), (3.12), leads to

$$\begin{aligned}\left[(M_2^2)(h_n(z)r_n(x)), \beta_n\right] = & i\omega_{n_1}(2h_{n2000}z_1^2 + h_{n1010}z_1z_3 + h_{n1001}z_1z_4 \\ & - 2h_{n0200}z_2^2 - h_{n0101}z_2z_4 - h_{n0110}z_2z_3) \\ & + i\omega_{n_2}(2h_{n0020}z_3^2 + h_{n1010}z_1z_3 + h_{n0110}z_2z_3 \\ & - 2h_{n0002}z_4^2 - h_{n1001}z_1z_4 - h_{n0101}z_2z_4) - \mathscr{M}_n h_n(z),\end{aligned} \tag{3.42}$$

where $\mathscr{M}_n$ is defined in (3.9). According to (3.10), (3.12), (3.30), we have that,

$$\begin{aligned}\tilde{f}_2^2(z,0,0) = & (I-\pi)\tilde{F}_2(\Phi z_x, 0) \\ = & \tilde{F}_2(\Phi z_x, 0) - (\psi_1^T[\tilde{F}_2(\Phi z_x, 0), \beta_{n_1}]\phi_1 + \overline{\psi_1}^T[\tilde{F}_2(\Phi z_x, 0), \beta_{n_1}]\overline{\phi_1})r_{n_1}(x) \\ & - (\psi_3^T[\tilde{F}_2(\Phi z_x, 0), \beta_{n_2}]\phi_3 + \overline{\psi_3}^T[\tilde{F}_2(\Phi z_x, 0), \beta_{n_2}]\overline{\phi_3})r_{n_2}(x), \\ \tilde{F}_2(\Phi z_x, 0) = & G_2^{d(0,0)}(\Phi z_x) + F_2(\Phi z_x, 0),\end{aligned}$$

which, combining (3.33), induces that, for $n_1 = 0,\ n_2 \neq 0$,

$$\begin{aligned}\left[\tilde{f}_2^2(z,0,0), \beta_0\right] = & \frac{1}{\sqrt{l\pi}}\Big((F_{2000} - \psi_1^T F_{2000}\phi_1 - \overline{\psi_1}^T F_{2000}\overline{\phi_1})z_1^2 \\ & + (\overline{F_{2000}} - \psi_1^T \overline{F_{2000}\phi_1} - \overline{\psi_1}^T \overline{F_{2000}\phi_1})z_2^2 \\ & + (F_{1100} - \psi_1^T F_{1100}\phi_1 - \overline{\psi_1}^T F_{1100}\overline{\phi_1})z_1z_2 \\ & + (F_{0020} - E_1 - \psi_1^T(F_{0020} - E_1)\phi_1 - \overline{\psi_1}^T(F_{0020} - E_1)\overline{\phi_1})z_3^2 \\ & + (\overline{F_{0020}} - \overline{E_1} - \psi_1^T(\overline{F_{0020}} - \overline{E_1})\phi_1 - \overline{\psi_1}^T(\overline{F_{0020}} - \overline{E_1})\overline{\phi_1})z_4^2 \\ & + (F_{0011} - E_2 - \psi_1^T(F_{0011} - E_2)\phi_1 - \overline{\psi_1}^T(F_{0011} - E_2)\overline{\phi_1})z_3z_4\Big), \\ [\tilde{f}_2^2(z,0,0), \beta_{n_2}] = & \frac{1}{\sqrt{l\pi}}\Big((F_{1010} - \psi_3^T F_{1010}\phi_3 - \overline{\psi_3}^T F_{1010}\overline{\phi_3})z_1z_3 \\ & + (F_{1001} - \psi_3^T F_{1001}\phi_3 - \overline{\psi_3}^T F_{1001}\overline{\phi_3})z_1z_4 \\ & + (\overline{F_{1001}} - \psi_3^T \overline{F_{1001}}\phi_3 - \overline{\psi_3}^T \overline{F_{1001}\phi_3})z_2z_3 \\ & + (\overline{F_{1010}} - \psi_3^T \overline{F_{1010}}\phi_3 - \overline{\psi_3}^T \overline{F_{1010}\phi_3})z_2z_4\Big), \\ [\tilde{f}_2^2(z,0,0), \beta_{2n_2}] = & \frac{1}{\sqrt{2l\pi}}\left((F_{0020} + E_1)z_3^2 + (\overline{F_{0020}} + \overline{E_1})z_4^2 + (F_{0011} + E_2)z_3z_4\right),\end{aligned} \tag{3.43}$$

where $E_1,\ E_2$ are defined by (3.34).

For $0 < n_1 < n_2$,

$$\begin{aligned}& \left[\tilde{f}_2^2(z,0,0), \beta_n\right] \\ & = \begin{cases}\frac{1}{\sqrt{l\pi}}\left((F_{2000} - E_5)z_1^2 + (\overline{F_{2000}} - \overline{E_5})z_2^2 + (F_{0020} - E_1)z_3^2\right. \\ \left. + (\overline{F_{0020}} - \overline{E_1})z_4^2 + (F_{1100} - E_6)z_1z_2 + (F_{0011} - E_2)z_3z_4\right), & n = 0, \\ \frac{1}{\sqrt{2l\pi}}\left((F_{0020} + E_1)z_3^2 + (\overline{F_{0020}} + \overline{E_1})z_4^2 + (F_{0011} + E_2)z_3z_4\right), & n = 2n_2,\end{cases}\end{aligned} \tag{3.44}$$

$$\left[\tilde{f}_2^2(z,0,0),\beta_n\right] = \begin{cases} \frac{1}{\sqrt{2l\pi}}\big((F_{1010}+E_3)z_1z_3+(\overline{F_{1010}}+\overline{E_3})z_2z_4 \\ +(F_{1001}+E_4)z_1z_4+(\overline{F_{1001}}+\overline{E_4})z_2z_3\big), & n=n_1+n_2, \\ \frac{1}{\sqrt{2l\pi}}\big((F_{1010}-E_3)z_1z_3+(\overline{F_{1010}}-\overline{E_3})z_2z_4 \\ +(F_{1001}-E_4)z_1z_4+(\overline{F_{1001}}-\overline{E_4})z_2z_3\big), & n=n_2-n_1,\ n_2\neq 2n_1,\ n_2\neq 3n_1, \\ \frac{1}{\sqrt{2l\pi}}\Big((F_{1010}-E_3-\psi_1^T(F_{1010}-E_3)\phi_1-\overline{\psi_1}^T(F_{1010}-E_3)\overline{\phi_1}))z_1z_3 \\ +(F_{1001}-E_4-\psi_1^T(F_{1001}-E_4)\phi_1-\overline{\psi_1}^T(F_{1001}-E_4)\overline{\phi_1}))z_1z_4 \\ +(\overline{F_{1001}}-\overline{E_4}-\psi_1^T(\overline{F_{1001}}-\overline{E_4})\phi_1-\overline{\psi_1}^T(\overline{F_{1001}}-\overline{E_4})\overline{\phi_1}))z_2z_3 \\ +(\overline{F_{1010}}-\overline{E_3}-\psi_1^T(\overline{F_{1010}}-\overline{E_3})\phi_1-\overline{\psi_1}^T(\overline{F_{1010}}-\overline{E_3})\overline{\phi_1}))z_2z_4\Big), & n=n_2-n_1,\ n_2=2n_1, \\ \frac{1}{\sqrt{2l\pi}}\big((F_{2000}+E_5)z_1^2+(\overline{F_{2000}}+\overline{E_5})z_2^2+(F_{1100}+E_6)z_1z_2 \\ +(F_{1010}-E_3)z_1z_3+(F_{1001}-E_4)z_1z_4+(\overline{F_{1010}}-\overline{E_3})z_2z_4 \\ +(\overline{F_{1001}}-\overline{E_4})z_2z_3\big), & n=n_2-n_1,\ n_2=3n_1, \end{cases} \tag{3.45}$$

and

$$\left[\tilde{f}_2^2(z,0,0),\beta_n\right] = \begin{cases} \frac{1}{\sqrt{2l\pi}}\Big((F_{2000}+E_5)z_1^2+(\overline{F_{2000}}\Big) \\ +\frac{1}{\sqrt{2l\pi}}\Big(\overline{E_5})z_2^2+(F_{1100}+E_6)z_1z_2\Big), & n=2n_1,\ n_2\neq 2n_1,\ n_2\neq 3n_1, \\ \frac{1}{\sqrt{2l\pi}}\Big((F_{2000}+E_5-\psi_3^T(F_{2000}+E_5)\phi_3-\overline{\psi_3}^T(F_{2000}+E_5)\overline{\phi_3})z_1^2 \\ +(\overline{F_{2000}}+\overline{E_5}-\psi_3^T(\overline{F_{2000}}+\overline{E_5})\phi_3-\overline{\psi_3}^T(\overline{F_{2000}}+\overline{E_5})\overline{\phi_3})z_2^2 \\ +(F_{1100}+E_6-\psi_3^T(F_{1100}+E_6)\phi_3-\overline{\psi_3}^T(F_{1100}+E_6)\overline{\phi_3})z_1z_2\Big), & n=2n_1, n_2=2n_1, \\ \frac{1}{\sqrt{2l\pi}}\big((F_{2000}+E_5)z_1^2+(\overline{F_{2000}}+\overline{E_5})z_2^2+(F_{1100}+E_6)z_1z_2 \\ +(F_{1010}+E_3)z_1z_3+(F_{1001}+E_4)z_1z_4+(\overline{F_{1010}}+\overline{E_3})z_2z_4 \\ +(\overline{F_{1001}}+\overline{E_3})z_2z_4\big), & n=2n_1,\ n_2=3n_1. \end{cases} \tag{3.46}$$

From (3.28), we have that,

$$[(M_2^2)(h_n(z)r_n(x)),\beta_n]=[\tilde{f}_2^2(z,0,0),\beta_n],\ n=0,1,2,\dots. \tag{3.47}$$

Next, we compute $h_{nq_1q_2q_3q_4}$ in three cases.

Case 1. For $n_1=0,\ n_2\neq 0$, from (3.42),(3.43), (3.47) and matching the coefficients $z_1^2,\ z_3^2,\ z_1z_2,\ z_3z_4$, we have that,

$$n=0,\begin{cases} 2i\omega_{n_1}h_{02000}-\mathscr{M}_0h_{02000}=\frac{1}{\sqrt{l\pi}}(F_{2000}-\psi_1^TF_{2000}\phi_1-\overline{\psi_1}^TF_{2000}\overline{\phi_1}), \\ 2i\omega_{n_2}h_{00020}-\mathscr{M}_0h_{00020}=\frac{1}{\sqrt{l\pi}}(F_{0020}-E_1-\psi_1^T(F_{0020}-E_1)\phi_1-\overline{\psi_1}^T(F_{0020}-E_1)\overline{\phi_1}), \\ -\mathscr{M}_0h_{01100}=\frac{1}{\sqrt{l\pi}}(F_{1100}-\psi_1^TF_{1100}\phi_1-\overline{\psi_1}^TF_{1100}\overline{\phi_1}), \\ -\mathscr{M}_0h_{00011}=\frac{1}{\sqrt{l\pi}}(F_{0011}-E_2-\psi_1^T(F_{0011}-E_2)\phi_1-\overline{\psi_1}^T(F_{0011}-E_2)\overline{\phi_1}). \end{cases}$$

Therefore,

$$\begin{cases} h_{02000} = \frac{1}{\sqrt{l\pi}}(2i\omega_{n_1}I - \mathscr{M}_0)^{-1}(F_{2000} - \psi_1^T F_{2000}\phi_1 - \overline{\psi_1}^T F_{2000}\overline{\phi_1}), \\ h_{00020} = \frac{1}{\sqrt{l\pi}}(2i\omega_{n_2}I - \mathscr{M}_0)^{-1}(F_{0020} - E_1 - \psi_1^T (F_{0020} - E_1)\phi_1 - \overline{\psi_1}^T (F_{0020} - E_1)\overline{\phi_1}), \\ h_{01100} = -\frac{1}{\sqrt{l\pi}}\mathscr{M}_0^{-1}(F_{1100} - \psi_1^T F_{1100}\phi_1 - \overline{\psi_1}^T F_{1100}\overline{\phi_1}), \\ h_{00011} = -\frac{1}{\sqrt{l\pi}}\mathscr{M}_0^{-1}(F_{0011} - E_2 - \psi_1^T (F_{0011} - E_2)\phi_1 - \overline{\psi_1}^T (F_{0011} - E_2)\overline{\phi_1}). \end{cases}$$

Similarly, when $n = n_2$ and $n = 2n_2$, by matching the coefficients $z_1z_3,\ z_1z_4,\ z_2z_3$, we have that,

$$\begin{cases} h_{n_2 1010} = \frac{1}{\sqrt{l\pi}}(i(\omega_{n_1} + \omega_{n_2})I - \mathscr{M}_{n_2})^{-1}(F_{1010} - \psi_3^T F_{1010}\phi_3 - \overline{\psi_3}^T F_{1010}\overline{\phi_3}), \\ h_{n_2 1001} = \frac{1}{\sqrt{l\pi}}(i(\omega_{n_1} - \omega_{n_2})I - \mathscr{M}_{n_2})^{-1}(F_{1001} - \psi_3^T F_{1001}\phi_3 - \overline{\psi_3}^T F_{1001}\overline{\phi_3}), \\ h_{n_2 0110} = \frac{1}{\sqrt{l\pi}}(i(\omega_{n_2} - \omega_{n_1})I - \mathscr{M}_{n_2})^{-1}(\overline{F_{1001}} - \psi_3^T \overline{F_{1001}}\phi_3 - \overline{\psi_3}^T \overline{F_{1001}\phi_3}), \\ h_{(2n_2)0011} = -\frac{1}{\sqrt{2l\pi}}\mathscr{M}_{2n_2}^{-1}(F_{0011} + E_2), \\ h_{(2n_2)0020} = \frac{1}{\sqrt{2l\pi}}(2i\omega_{n_2}I - \mathscr{M}_{2n_2})^{-1}(F_{0020} + E_1), \quad h_{(2n_2)1100} = \vec{0}. \end{cases}$$

Case 2. For $0 < n_1 < n_2$, from (3.42), (3.44), (3.46), (3.47) and matching the coefficients $z_1^2,\ z_3^2,\ z_1z_2,\ z_3z_4$, we have that,

$$n = 0, \begin{cases} 2i\omega_{n_1}h_{02000} - \mathscr{M}_0 h_{02000} = \frac{1}{\sqrt{l\pi}}(F_{2000} - E_5), \\ 2i\omega_{n_2}h_{00020} - \mathscr{M}_0 h_{00020} = \frac{1}{\sqrt{l\pi}}(F_{0020} - E_1), \\ -\mathscr{M}_0 h_{01100} = \frac{1}{\sqrt{l\pi}}(F_{1100} - E_6), \\ -\mathscr{M}_0 h_{00011} = \frac{1}{\sqrt{l\pi}}(F_{0011} - E_2). \end{cases}$$

Therefore,

$$\begin{cases} h_{02000} = \frac{1}{\sqrt{l\pi}}(2i\omega_{n_1}I - \mathscr{M}_0)^{-1}(F_{2000} - E_5), \\ h_{00020} = \frac{1}{\sqrt{l\pi}}(2i\omega_{n_2}I - \mathscr{M}_0)^{-1}(F_{0020} - E_1), \\ h_{01100} = -\frac{1}{\sqrt{l\pi}}\mathscr{M}_0^{-1}(F_{1100} - E_6), \\ h_{00011} = -\frac{1}{\sqrt{l\pi}}\mathscr{M}_0^{-1}(F_{0011} - E_2). \end{cases}$$

Similarly, when $n = 2n_1,\ n = n_1 + n_2,\ n = n_2 - n_1$ and $n = 2n_2$, by matching the coefficients $z_1^2,\ z_3^2,\ z_1z_2,\ z_1z_3,\ z_1z_4,\ z_2z_3,\ z_3z_4$, we have that,

$$n = 2n_2, \begin{cases} h_{(2n_2)0011} = -\frac{1}{\sqrt{2l\pi}}\mathscr{M}_{2n_2}^{-1}(F_{0011} + E_2), \\ h_{(2n_2)0020} = \frac{1}{\sqrt{2l\pi}}(2i\omega_{n_2}I - \mathscr{M}_{2n_2})^{-1}(F_{0020} + E_1), \quad h_{(2n_2)1100} = \vec{0}, \end{cases}$$

$$n = n_1 + n_2, \begin{cases} h_{(n_1+n_2)1001} = \frac{1}{\sqrt{2l\pi}}(i(\omega_{n_1} - \omega_{n_2})I - \mathscr{M}_{n_1+n_2})^{-1}(F_{1001} + E_4), \\ h_{(n_1+n_2)0110} = \frac{1}{\sqrt{2l\pi}}(i(\omega_{n_2} - \omega_{n_1})I - \mathscr{M}_{n_1+n_2})^{-1}(\overline{F_{1001}} + \overline{E_4}), \\ h_{(n_1+n_2)1010} = \frac{1}{\sqrt{2l\pi}}(i(\omega_{n_2} + \omega_{n_1})I - \mathscr{M}_{n_1+n_2})^{-1}(F_{1010} + E_3). \end{cases}$$

For $n = 2n_1,\ n_2 \neq 2n_1$,

$$\begin{cases} h_{(2n_1)1100} = -\frac{1}{\sqrt{2l\pi}}(\mathscr{M}_{2n_1})^{-1}(F_{1100} + E_6), & h_{(2n_1)0011} = \vec{0}, \\ h_{(2n_1)2000} = \frac{1}{\sqrt{2l\pi}}(2i\omega_{n_1}I - \mathscr{M}_{2n_1})^{-1}(F_{2000} + E_5), & h_{(2n_1)0020} = \vec{0}. \end{cases}$$

For $n = 2n_1,\ n_2 = 2n_1$,

$$\begin{cases} h_{(2n_1)1100} = -\frac{1}{\sqrt{2l\pi}}(\mathscr{M}_{2n_1})^{-1}(F_{1100} + E_6 - \psi_3^T(F_{1100} + E_6)\phi_3 - \overline{\psi_3}^T(F_{1100} + E_6)\overline{\phi_3}), \\ h_{(2n_1)2000} = \frac{1}{\sqrt{2l\pi}}(2i\omega_{n_1} I - \mathscr{M}_{2n_1})^{-1}(F_{2000} + E_5 - \psi_3^T(F_{2000} + E_5)\phi_3 - \overline{\psi_3}^T(F_{2000} + E_5)\overline{\phi_3}), \\ h_{(2n_1)0011} = h_{(2n_1)0020} = \vec{0}. \end{cases}$$

For $n = n_2 - n_1,\ n_2 \neq 2n_1$,

$$\begin{cases} h_{(n_2-n_1)1001} = \frac{1}{\sqrt{2l\pi}}(i(\omega_{n_1} - \omega_{n_2})I - \mathscr{M}_{n_2-n_1})^{-1}(F_{1001} - E_4), \\ h_{(n_2-n_1)1010} = \frac{1}{\sqrt{2l\pi}}(i(\omega_{n_1} + \omega_{n_2})I - \mathscr{M}_{n_2-n_1})^{-1}(F_{1010} - E_3), \\ h_{(n_2-n_1)0110} = \frac{1}{\sqrt{2l\pi}}(i(\omega_{n_2} - \omega_{n_1})I - \mathscr{M}_{n_2-n_1})^{-1}(\overline{F_{1001}} - \overline{E_4}). \end{cases}$$

For $n = n_2 - n_1,\ n_2 = 2n_1$,

$$\begin{cases} h_{(n_2-n_1)1001} = & \frac{1}{\sqrt{2l\pi}}(i(\omega_{n_1} - \omega_{n_2})I - \mathscr{M}_{n_2-n_1})^{-1}(F_{1001} - E_4 \\ & -\psi_1^T(F_{1001} - E_4)\phi_1 - \overline{\psi_1}^T(F_{1001} - E_4)\overline{\phi_1})), \\ h_{(n_2-n_1)1010} = & \frac{1}{\sqrt{2l\pi}}(i(\omega_{n_1} + \omega_{n_2})I - \mathscr{M}_{n_2-n_1})^{-1}(F_{1010} - E_3 \\ & -\psi_1^T(F_{1010} - E_3)\phi_1 - \overline{\psi_1}^T(F_{1010} - E_3)\overline{\phi_1})), \\ h_{(n_2-n_1)0110} = & \frac{1}{\sqrt{2l\pi}}(i(\omega_{n_2} - \omega_{n_1})I - \mathscr{M}_{n_2-n_1})^{-1}(\overline{F_{1001}} - \overline{E_4} \\ & -\psi_1^T(\overline{F_{1001}} - \overline{E_4})\phi_1 - \overline{\psi_1}^T(\overline{F_{1001}} - \overline{E_4})\overline{\phi_1})). \end{cases}$$

Hence, by (3.21), (3.26), (3.27), (3.29), (3.35) and (3.41), the norm form to third order for double bifurcation is as follows:

$$\dot{z} = Bz + \begin{pmatrix} B_{n_1 1}z_1\epsilon_1 + B_{n_1 2}z_1\epsilon_2 \\ \overline{B_{n_1 1}}z_2\epsilon_1 + \overline{B_{n_1 2}}z_2\epsilon_2 \\ B_{n_2 1}z_3\epsilon_1 + B_{n_2 2}z_3\epsilon_2 \\ \overline{B_{n_2 1}}z_4\epsilon_1 + \overline{B_{n_2 2}}z_4\epsilon_2 \end{pmatrix} + \begin{pmatrix} B_{2100}z_1^2 z_2 + B_{1011}z_1 z_3 z_4 \\ \overline{B_{2100}}z_1 z_2^2 + \overline{B_{1011}}z_2 z_3 z_4 \\ B_{0021}z_3^2 z_4 + B_{1110}z_1 z_2 z_3 \\ \overline{B_{0021}}z_3 z_4^2 + \overline{B_{1110}}z_1 z_2 z_4 \end{pmatrix}, \tag{3.48}$$

where,

$$\begin{aligned} B_{2100} &= C_{2100} + \frac{3}{2}(D_{2100} + E_{2100}), \quad B_{1011} = C_{1011} + \frac{3}{2}(D_{1011} + E_{1011}), \\ B_{0021} &= C_{0021} + \frac{3}{2}(D_{0021} + E_{0021}), \quad B_{1110} = C_{1110} + \frac{3}{2}(D_{1110} + E_{1110}). \end{aligned}$$

Making double polar coordinates transformation by

$$z_1 = \rho_1 e^{i\theta_1},\ z_2 = \rho_1 e^{-i\theta_1},\ z_3 = \rho_2 e^{i\theta_2},\ z_4 = \rho_2 e^{-i\theta_2},$$

system (3.48) is equivalent to the following equation:

$$\begin{aligned} \dot{\rho}_1 &= \rho_1(c_1\epsilon_1 + c_2\epsilon_2 + d_1\rho_1^2 + k_1\rho_2^2), \\ \dot{\rho}_2 &= \rho_2(c_3\epsilon_1 + c_4\epsilon_2 + d_2\rho_1^2 + k_2\rho_2^2), \end{aligned}$$

where

$$\begin{aligned} &c_1 = Re(B_{n_1 1}),\ c_2 = Re(B_{n_1 2}),\ c_3 = Re(B_{n_2 1}),\ c_4 = Re(B_{n_2 2}), \\ &d_1 = Re(B_{2100}),\ d_2 = Re(B_{1110}),\ k_1 = Re(B_{1011}),\ k_2 = Re(B_{0021}). \end{aligned}$$

4 Numerical Simulations

In this section, we numerically investigate the spatiotemporal patterns of system (2.12). Firstly, for the local system (2.16) with

$$r = 1,\ k = 2,\ \beta = 1.2,\ \gamma = 1,\ \xi = 2,\ \eta = 0.5,$$

it follows from $(A1)$ that the positive equilibrium E_2 exists for $0 < \rho < 2/(2\sigma + 1)$ and from (2.17) that system (2.16) has no Hopf bifurcation for $\rho > \rho^*_{max} \approx 0.3431$. By (2.15), we have the Hopf bifurcation curve H: $\rho = (2\sigma - 1)/(2\sigma^2 + \sigma)$ and E_2 is asymptotically stable for $\rho > (2\sigma - 1)/(2\sigma^2 + \sigma)$ and unstable for $\rho < (2\sigma - 1)/(2\sigma^2 + \sigma)$. The stability region D_1 and the Hopf bifurcation curve H for system (2.16) in the σ–ρ plane are illustrated in Fig. 1a for $0 < \sigma < 4.2$ and $0 < \rho < 2$.

For fixed $\rho = 0.2 < \rho^*_{max}$, we have $\sigma_1 \simeq 0.6492$ and $\sigma_2 \simeq 3.8508$. Thus, the positive equilibrium E_2 is asymptotically stable for $0 < \sigma < \sigma_1$ or $\sigma > \sigma_2$ and unstable for $\sigma_1 < \sigma < \sigma_2$, and system (2.16) undergoes Hopf bifurcations at $\sigma = \sigma_j$, $j = 1, 2$, which are also the critical values of the spatially homogeneous Hopf bifurcation of the diffusive system (2.12). Then, for (2.12), choosing the diffusive coefficients and the spatial interval $(0, l\pi)$ as

$$\delta_N = 0.5,\ \delta_P = 0.8,\ \delta_S = 0.5,\ l = 4,$$

we investigate the spatiotemporal dynamics taking the parameters χ and σ as two bifurcation parameters. It follows from Lemma 2.2 that $[\sqrt{x_0}l] = 1$ if $\sigma \in (0, 4.2)$. A further calculation shows that $\chi_1^H(\sigma) > \chi_2^H(\sigma)$ for $\sigma \in (0, 0.1837) \cup (4.0146, 4.2)$ and $\chi_1^H(\sigma) < \chi_2^H(\sigma)$ for $\sigma \in (0.1837, 4.0146)$. Thus,

$$n_H^* = \begin{cases} 1, & \sigma \in (0.1837, 4.0146), \\ 2, & \sigma \in (0, 0.1837) \cup (4.0146, 4.2). \end{cases}$$

Denote the Hopf bifurcation curves in the σ–χ plane by

$$H_0^{(1)} : \sigma = \sigma_1 \simeq 0.6492,\quad H_0^{(2)} : \sigma = \sigma_2 \simeq 3.8508,$$

which correspond to the spatially homogeneous Hopf bifurcations, and by Theorem 2.1,

$$H_1 : \chi = \chi_1^H(\sigma) = \frac{2.5(1 - 0.2\sigma)^2(9.3a_{11}^2 - (9.4429 - 0.768\sigma)a_{11} + 0.7058 - 0.0624\sigma)}{0.9 - 0.2\sigma},$$
$$H_2 : \chi = \chi_2^H(\sigma) = \frac{2.5(1 - 0.2\sigma)^2(3.3a_{11}^2 - (4.4115 - 0.192\sigma)a_{11} + 1.0852 - 0.0624\sigma)}{0.9 - 0.2\sigma},$$

where $a_{11} = 0.2(\sigma + 0.5 - 1/(1 - 0.2\sigma))$, which correspond to the spatially inhomogeneous Hopf bifurcations, for wave numbers $n = 1$ and $n = 2$, respectively.

Similarly, by Lemma 2.3, we have

$$n_T^* = \begin{cases} 3, & \sigma \in (0, 2.857), \\ 2, & \sigma \in (2.857, 4.2). \end{cases}$$

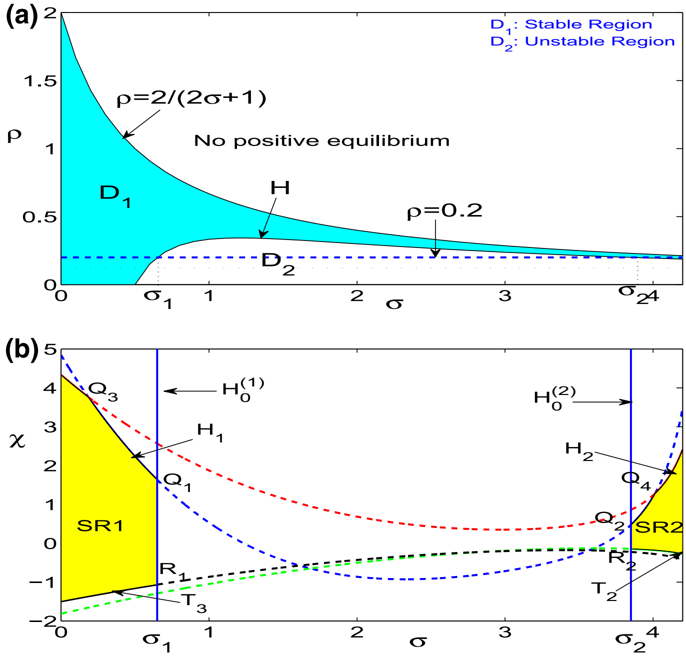

Fig. 1 **a** The existence and stability regions of the positive equilibrium E_2 of the local system (2.16); **b** Stability regions and bifurcation diagrams for the diffusive system (2.12) in the $\chi - \sigma$ for $\rho = 0.2$ and other parameters are the same as in (**a**). The shaded regions $SR1$ and $SR2$ are stable regions, $H_0^{(1)}$ and $H_0^{(2)}$ are homogeneous Hopf bifurcation lines. H_1, H_2 are spatially inhomogeneous Hopf bifurcation curves and T_3, T_2 are critical Turing bifurcation curves

Then, by Theorems 2.1 and 2.2, the boundaries of the stability regions of system (2.12) consist of the spatially inhomogeneous Hopf bifurcation curves H_1 and H_2, the spatially homogeneous Hopf bifurcation lines $H_0^{(1)}$ and $H_0^{(2)}$ and the Turing bifurcation curves T_3 and T_2, as shown in Fig. 1b, where

$$T_2 : \chi = \chi_2^T(\sigma) = -\frac{2.5(1-0.2\sigma)^2}{0.9-0.2\sigma}\left(-0.22\sigma + 0.5525 + \frac{1}{10-2\sigma}\right),$$

$$T_3 : \chi = \chi_3^T(\sigma) = -\frac{2.5(1-0.2\sigma)^2}{0.9-0.2\sigma}\left(-0.1917\sigma + 0.4133 + \frac{0.125}{1-0.2\sigma}\right),$$

according to Theorem 2.2.

The spatially inhomogeneous Hopf bifurcation curves H_1 and H_2 intersect at two points $Q_3(0.1837, 3.7633)$ and $Q_4(4.0146, 1.2837)$. The spatially inhomogeneous Hopf bifurcation curve H_1 intersects with the straight Hopf bifurcation lines $H_0^{(1)}$ and $H_0^{(2)}$ at the point $Q_1(0.6492, 1.6353)$ and $Q_2(3.8508, 0.4736)$, respectively. These double-Hopf bifurcation points Q_j, $(j = 1, 2, 3, 4)$ lie on the the boundaries of the stability regions of system (2.12).

The critical Turing bifurcation curves T_3 and T_2 intersect with the straight Hopf bifurcation lines $H_0^{(1)}$ and $H_0^{(2)}$ at the points $R_1(0.6492, -1.063)$ and $R_2(3.8508, -0.1428)$, respectively. By Theorem 2.5, system (2.12) undergoes Turing–Hopf bifurcations near the positive constant equilibrium E_2 at R_1 and R_2, which also lie on the the boundaries of the stability regions of system (2.12).

In what follows, we are interested in the dynamical classification of system (2.12) near the double-Hopf bifurcation points.

4.1 The Double-Hopf Bifurcations Due to the Intersection of the Spatially Homogeneous and Inhomogeneous Hopf Bifurcations

For the double-Hopf bifurcation point $Q_2(3.8508, 0.4736)$, which is the intersection point of the spatially homogeneous Hopf bifurcation line $H_0^{(2)}$ and the spatially inhomogeneous Hopf bifurcation curves H_1, we have $n_1 = 0,\ n_2 = 1$ and it follows from (2.5) and (2.8) that

$$\omega_0 = 0.1765, \quad \omega_1 = 0.2755.$$

Letting $\epsilon_1 = \sigma - 3.8508,\ \epsilon_2 = \chi - 0.4736$ and employing the procedure developed in Sect. 3, we obtain the normal form truncated to the third order terms as follows:

$$\begin{cases} \dot{\rho}_1 = \rho_1(-0.2786\epsilon_1 - 0.03075\rho_1^2 - 10.0633\rho_2^2), \\ \dot{\rho}_2 = \rho_2(-0.2396\epsilon_1 + 0.0681\epsilon_2 - 0.0464\rho_1^2 - 0.057\rho_2^2). \end{cases} \tag{4.1}$$

System (4.1) has a zero equilibrium $E_0^*(0, 0)$ for any $\epsilon_1,\ \epsilon_2 \in R$, and two boundary equilibria

$$E_1^*(\sqrt{-9.0594\epsilon_1}, 0),\ \epsilon_1 < 0;\ E_2^*(0, \sqrt{-4.2006\epsilon_1 + 1.1943\epsilon_2}),\ \epsilon_2 > 3.5173\epsilon_1,$$

and a positive equilibrium

$$E^*(\sqrt{-5.1462\epsilon_1 + 1.4728\epsilon_2}, \sqrt{-0.01196\epsilon_1 - 0.00401\epsilon_2}),\ 3.4941\epsilon_1 < \epsilon_2 < -2.6569\epsilon_1.$$

By analyzing the stability and bifurcation of these equilibria, the normal form (4.1) is the so-called simple case, illustrated in [28]. The phase portrait is easy to be obtained in Fig. 2, where the curves $H_0^{(2)},\ \widetilde{H}_1,\ L_2^1,\ L_2^2$ are denoted by

$$\begin{aligned} &H_0^{(2)}:\ \sigma = 3.8508,\ \widetilde{H}_1:\ \chi = 0.4736 + 3.5173(\sigma - 3.8508), \\ &L_2^1:\ \chi = 0.4736 + 3.4941(\sigma - 3.8508),\ (\sigma < 3.8508), \\ &L_2^2:\ \chi = 0.4736 - 2.6569(\sigma - 3.8508),\ (\sigma < 3.8508). \end{aligned}$$

The lines $H_0^{(2)},\ \widetilde{H}_1,\ L_2^1,\ L_2^2$ divide the (σ, χ) plane into six regions with different dynamics.

Remark 4.1 The Hopf bifurcation line $\widetilde{H}_1$ obtained by the normal form (4.1) is tangent to the Hopf bifurcation curve H_1 due to the linear analysis at the point $Q_2(3.8508, 0.4736)$.

According to the phase portrait Fig. 2, there are three stable patterns near the double-Hopf bifurcation point Q_2 as follows:

(i) when $(\sigma, \chi) = (3.858, 0.44) \in$ ①, (4.1) has a stable equilibrium E_0^*, which implies that the positive equilibrium $E_2(0.8757, 2.0511, 3.5026)$ of system (2.12) is asymptotically stable, as shown in Fig. 3a, d;
(ii) when $(\sigma, \chi) = (3.848, 0.44) \in$ ⑥, (4.1) has a stable boundary equilibrium E_1^*, which implies that system (2.12) has a stable spatially homogeneous periodic solution, as shown in Fig. 3b, e;
(iii) when $(\sigma, \chi) = (3.8608, 0.5096) \in$ ②, (4.1) has a stable boundary equilibrium E_2^*, which implies that system (2.12) has a stable spatially inhomogeneous periodic solution with the spatial shape like $\cos(x/4)$, as shown in Fig. 3c, f.

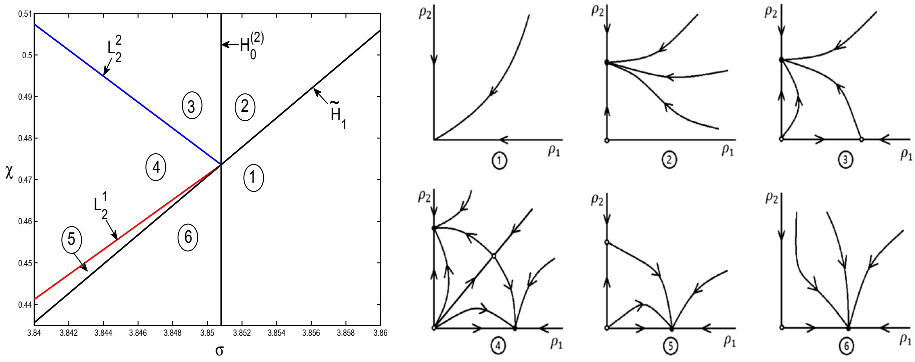

Fig. 2 The phase portrait near the double-Hopf bifurcation point Q_2 in Fig. 1

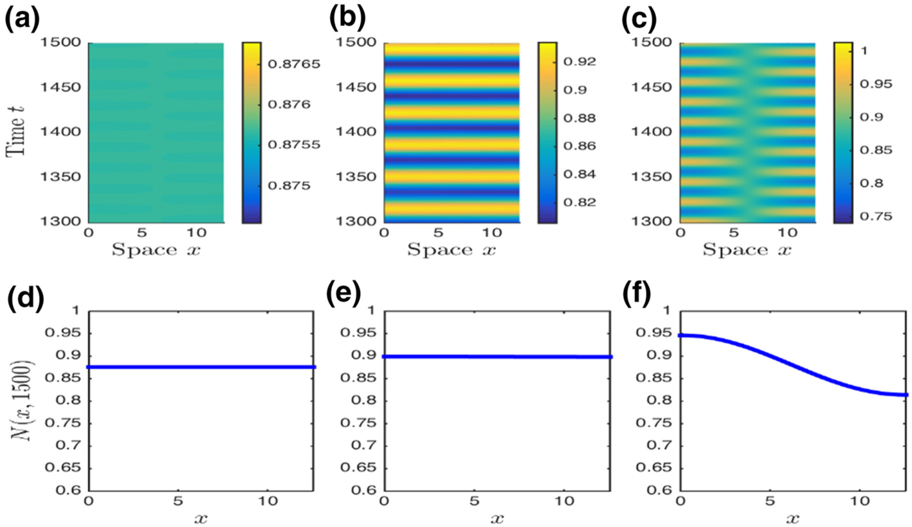

Fig. 3 Spatiotemporal dynamics of (2.12) for different parameters σ and χ near the point Q_2: **a**, **b** and **c** are the projections of $N(x, t)$ on the x–t plane for $(\sigma, \chi) = (3.858, 0.44) \in$ ①, $(\sigma, \chi) = (3.848, 0.44) \in$ ⑥, $(\sigma, \chi) = (3.8608, 0.5096) \in$ ②, respectively. **d**, **e** and **f** are the spatial profiles for fixed time $t = 1500$ of (**a**), (**b**) and (**c**), respectively

Except for these stable patterns, there are two types of pattern transitions: (i) from unstable spatially homogeneous periodic solution to stable spatially inhomogeneous periodic solution, which exists in the region ③, (see Fig. 4a); (ii) from unstable spatially inhomogeneous periodic solution to stable spatially homogeneous periodic solution, which exists in the region ⑤, (see Fig. 5a). Figures 4a and 5a are the projections of $N(x, t)$ on the x–t plane for $(\sigma, \chi) = (3.85, 0.49) \in$ ③ and $(\sigma, \chi) = (3.842, 0.4438) \in$ ⑤, respectively. Figure 4b, c are the truncated sections of Fig. 4a for short-term and long-term behaviors, respectively. Figure 5b, c are the truncated sections of Fig. 5a for short-term and long-term behaviors, respectively.

When (σ, χ) lies in the region ④, two stable spatially homogeneous and inhomogeneous periodic solutions coexist.

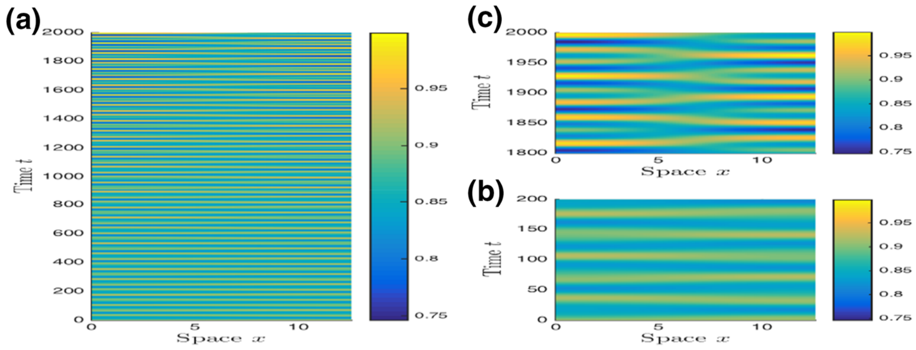

Fig. 4 **a** The projection of $N(x,t)$ on the x–t plane for $(\sigma, \chi) = (3.85, 0.49) \in$ ③, which shows the existence of the pattern transition from unstable spatially homogeneous periodic solution to stable spatially inhomogeneous periodic solution. **b** and **c** are the truncated section of (**a**) for short-term and long-term behaviors, respectively

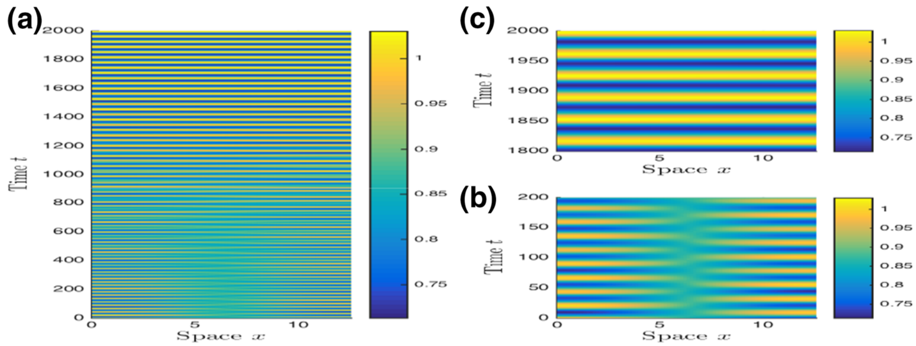

Fig. 5 **a** The projection of $N(x,t)$ on the x–t plane for $(\sigma, \chi) = (3.842, 0.4438) \in$ ⑤, which shows the existence of the pattern transition from unstable spatially inhomogeneous periodic solution to stable spatially homogeneous periodic solution. **b**, **c** are the truncated section of (**a**) for short-term and long-term behaviors, respectively

4.2 The double-Hopf bifurcations due to the intersection of two spatially inhomogeneous Hopf bifurcations

For the double-Hopf bifurcation point $Q_3(0.1837, 3.7633)$, which is the intersection point of two spatially inhomogeneous Hopf bifurcation curves H_1 and H_2, we have $n_1 = 1, n_2 = 2$ and $\omega_1 = 0.5414,\ \omega_2 = 0.7027$, and the normal form truncated to the third order terms is

$$\begin{cases} \dot{\rho}_1 = \rho_1(0.08387\epsilon_1 + 0.0153\epsilon_2 - 0.0902\rho_1^2 - 0.1524\rho_2^2), \\ \dot{\rho}_2 = \rho_2(0.08896\epsilon_1 + 0.03029\epsilon_2 + 0.1093\rho_1^2 - 0.1886\rho_2^2). \end{cases} \tag{4.2}$$

System (4.2) has a zero equilibrium $M_0(0,0)$ for any $\epsilon_1,\ \epsilon_2 \in R$, and two boundary equilibria

$$M_1(\sqrt{0.9296\epsilon_1 + 0.1696\epsilon_2}, 0),\ \epsilon_2 > -5.4822\epsilon_1;\ M_2(0, \sqrt{0.4716\epsilon_1 + 0.1605\epsilon_2}),\ \epsilon_2 > -2.9373\epsilon_1,$$

and a positive equilibrium

$$M(\sqrt{0.06715\epsilon_1 - 0.05138\epsilon_2}, \sqrt{0.5105\epsilon_1 + 0.1308\epsilon_2}),\ \text{for}\ -3.9033\epsilon_1 < \epsilon_2 < 1.3069\epsilon_1.$$

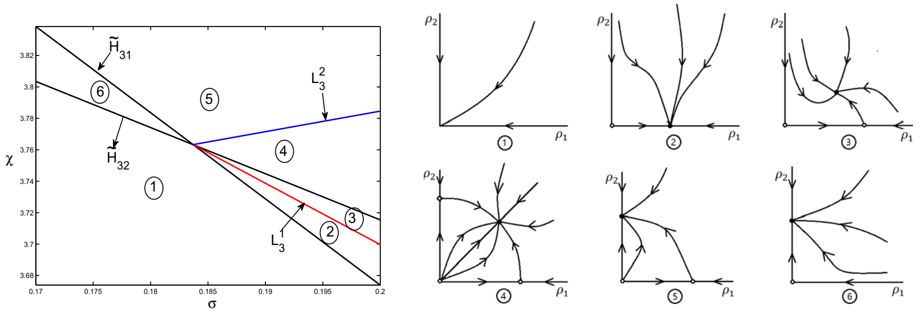

Fig. 6 The phase portrait near the double-Hopf bifurcation point Q_3 in Fig. 1

And the phase portrait for (4.2) is plotted in Fig. 6, where the curves $\widetilde{H}_{31},\ \widetilde{H}_{32},\ L_3^1,\ L_3^2$ are denoted by

$$\widetilde{H}_{31}:\ \chi = 3.7633 - 5.4822(\sigma - 0.1837),\ \widetilde{H}_{32}:\ \chi = 3.7633 - 2.9373(\sigma - 0.1837),$$
$$L_3^1:\ \chi = 3.7633 - 3.9033(\sigma - 0.1837),\ (\sigma > 0.1837),$$
$$L_3^2:\ \chi = 3.7633 + 1.3069(\sigma - 0.1837),\ (\sigma > 0.1837).$$

The lines $\widetilde{H}_{31},\ \widetilde{H}_{32},\ L_3^1,\ L_3^2$ divide the (σ,χ) plane into six regions with different dynamics.

Remark 4.2 The Hopf bifurcation curves $\widetilde{H}_{31}$ and $\widetilde{H}_{32}$ obtained by the normal form (4.2) are tangent to the Hopf bifurcation curves H_1 and H_2, respectively, due to the linear analysis at the point $Q_3(0.1837, 3.7633)$.

According to the phase portrait Fig. 6, there are four stable patterns near the double-Hopf bifurcation point Q_3:

(i) when $(\sigma,\chi) = (0.18, 3.685) \in$ ①, system (4.2) has a stable equilibrium M_0, which means that the positive equilibrium $E_2(0.2075, 0.7748, 0.8299)$ of system (2.12) is asymptotically stable, as shown in Fig. 7a, e;
(ii) when $(\sigma,\chi) = (0.19, 3.736) \in$ ②, system (4.2) has a stable boundary equilibrium M_1, which means that system (2.12) has a stable spatially inhomogeneous periodic solution with the spatial shape like $\cos(x/4)$, as shown in Fig. 7b, f;
(iii) when $(\sigma,\chi) = (0.18, 3.78) \in$ ⑥, system (4.2) has a stable boundary equilibrium M_2, which means that system (2.12) has a stable spatially inhomogeneous periodic solution with the spatial shape like $\cos(x/2)$, as shown in Fig. 7c, g;
(iv) when $(\sigma,\chi) = (0.19, 3.752) \in$ ④, system (4.2) has a stable positive equilibrium M and two unstable boundary equilibria $M_1,\ M_2$, which means that system (2.12) has a stable spatially inhomogeneous quasi-periodic solution with the spatial shape like the combination of $\cos(x/4)$ and $\cos(x/2)$, as shown in Fig. 7d, h.

For fixed space variable $x = \pi/5$, Fig. 8a–c are the time evolutions of $N(x,t)$, and (d), (e) and (f) are the orbits of system (2.12) in the phase space corresponding to Fig. 7b–d.

In addition, besides these four stable patterns, there are still three types of pattern transitions: (i) from unstable spatially inhomogeneous periodic solution with the spatial shape like $\cos(x/4)$ to stable spatially inhomogeneous quasi-periodic solution for $(\sigma,\chi) \in$ ③; (ii) from unstable spatially inhomogeneous periodic solution with the spatial shape like $\cos(x/2)$ to stable spatially inhomogeneous quasi-periodic solution for $(\sigma,\chi) \in$ ④; (iii)

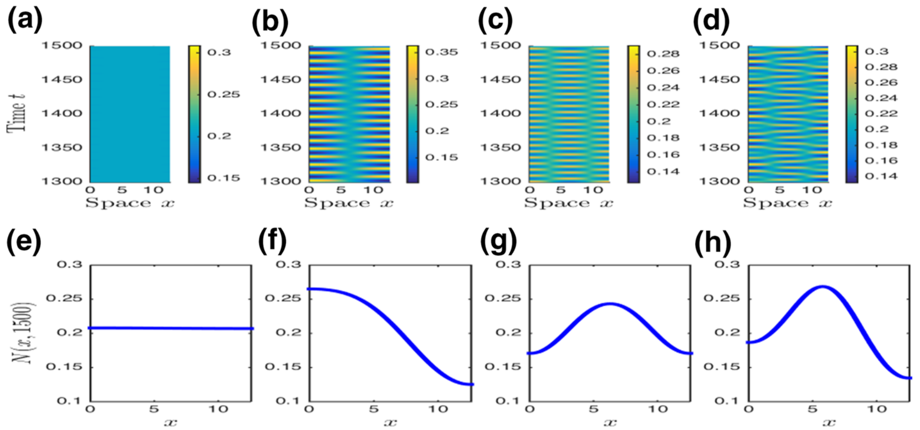

Fig. 7 Spatiotemporal dynamics of (2.12) for different parameters σ and χ near the point Q_3: **a**–**d** are the projections of $N(x,t)$ on the x–t plane for $(\sigma,\chi) = (0.18, 3.685) \in$ ①, $(\sigma,\chi) = (0.19, 3.736) \in$ ②, $(\sigma,\chi) = (0.18, 3.78) \in$ ⑥, $(\sigma,\chi) = (0.19, 3.752) \in$ ④, respectively. **e**–**h** are the spatial profiles for fixed time $t = 1500$ of **a**–**d**, respectively

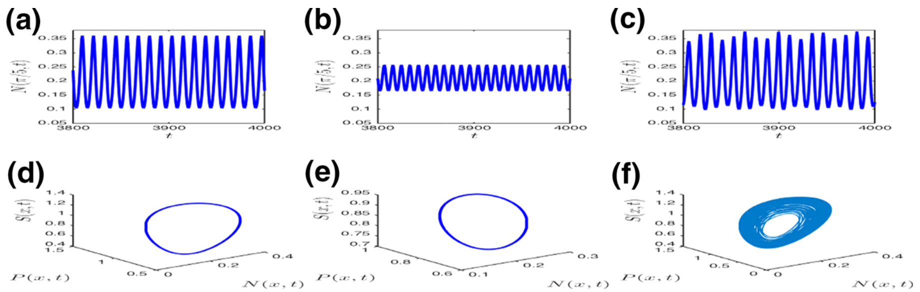

Fig. 8 For fixed space variable $x = \pi/5$, **a**–**c** are the time evolution of $N(x,t)$, and **d**–**f** are the orbit of system (2.12) in the phase space with the same parameters σ and χ as in Fig. 7b–d, respectively. **d**–**e** show the existence of stable periodic orbit and **f** shows the existence of the quasi-periodic orbit

from unstable spatially inhomogeneous periodic solution with the spatial shape like $\cos(x/4)$ to stable spatially inhomogeneous periodic solution with the spatial shape like $\cos(x/2)$ for $(\sigma,\chi) \in$ ⑤.

Remark 4.3 Compared with the case of Q_2, the stable spatially inhomogeneous quasi-periodic solution newly appears, but there is no the existence of stable spatially homogeneous and inhomogeneous periodic solutions.

5 Conclusion

In this paper, we investigate the effect of the indirect prey-taxis on the dynamics of the Gause–Kolmogorov-type predator–prey system. The stability of the positive equilibrium and the possible bifurcations are studied. We obtain the conditions guaranteeing the occurrence of the Hopf bifurcation, double-Hopf bifurcation and Turing–Hopf bifurcation and the explicit critical values for these bifurcations are determined.

For this system and under the assumption that the positive equilibrium of the corresponding ordinary differential system is stable, there is no diffusion-driven Turing instability when there is no indirect prey-taxis ($\chi = 0$). For the repulsive indirect taxis ($\chi < 0$), there exists only taxis-driven Turing bifurcation but no Hopf bifurcations and the boundaries of the stability region consist of the Turing bifurcation curves and the spatially homogeneous Hopf bifurcation curve. The intersection points of these boundary curves are Turing–Turing bifurcation and Turing–Hopf bifurcation points, which may result in the occurrence of the spatially inhomogeneous steady state, spatially homogeneous/inhomogeneous periodic solutions and the coexistence of multiple stable steady states.

For the attractive indirect taxis ($\chi > 0$), there exists only prey-taxis-driven spatially Hopf bifurcation but no Turing bifurcation, which do not occur for the reaction–diffusion predator–prey model with a direct prey-taxi like (1.1), and the boundaries of the stability region consist of the Hopf bifurcation curves. The intersection points of these boundary curves are double-Hopf bifurcation points, which leads to the occurrence of the spatially homogeneous/inhomogeneous periodic solutions and quasi-periodic solutions. To theoretically investigate the dynamical classification near the double-Hopf bifurcation point, we take the indirect prey-taxis and other parameter in the reaction term as the perturbation parameters, and then derive an algorithm for calculating the normal form of codimension-2 double-Hopf bifurcation for the non-resonance and weak resonance.

We also apply the obtained theoretical results to the system with the Holling-II functional response. The stable region and the bifurcation curves are completely determined in the $\sigma - \chi$ plane, where σ is the self saturation coefficient. Employing the normal form of the double-Hopf bifurcation, the dynamical classification near this double-Hopf bifurcation point is explicitly determined. For the double-Hopf bifurcation derived from the interaction of the spatially homogeneous and inhomogeneous Hopf bifurcations, there are three kinds of stable patterns: constant equilibrium, spatially homogeneous periodic solutions and spatially inhomogeneous periodic solutions. Except for these stable spatial–temporal patterns, there are two types of pattern transitions: one is from unstable spatially homogeneous periodic solution to stable spatially inhomogeneous periodic solution, the other is from unstable spatially inhomogeneous periodic solution to stable spatially homogeneous periodic solution.

For the double-Hopf bifurcation derived from the interaction of two spatially inhomogeneous Hopf bifurcations, there are four kinds of stable patterns: constant equilibrium, two kinds of spatially inhomogeneous periodic solutions with different spatial profiles and spatially inhomogeneous quasi-periodic solutions. Besides these four stable spatial–temporal patterns, there are pattern transitions either between two spatially inhomogeneous periodic solution with different spatial profiles or between spatially inhomogeneous periodic solution and spatially inhomogeneous quasi-periodic solution.

There are other interesting but challenging bifurcation problems worthy of investigation for this system with indirect prey-taxis: the spatial–temporal dynamics induced by the other codimension-two bifurcations such as Turing–Turing bifurcation and Turing–Hopf bifurcation or by the strong resonance double-Hopf bifurcation which may be the codimension-three bifurcation.

Acknowledgements We would like to thank the anonymous reviewer for his/her carefully reading the manuscript and many valuable and professional comments and suggestions, which greatly improve the initial manuscript.

References

1. Ahn, I., Yoon, C.: Global well-posedness and stability analysis of prey–predator model with indirect prey-taxis. J. Differ. Equ. **268**(8), 4222–4255 (2020)
2. Ainseba, B., Bendahmane, M., Noussair, A.: A reaction–diffusion system modeling predator–prey with prey-taxis. Nonlinear Anal. Real World Appl. **9**(5), 2086–2105 (2008)
3. Allesina, S., Tang, S.: Stability criteria for complex ecosystems. Nature **483**(7388), 205–208 (2012)
4. Arditi, R., Tyutyunov, Y., Morgulis, A., Govorukhin, V., Senina, I.: Directed movement of predators and the emergence of density-dependence in predator–prey models. Theor. Popul. Biol. **59**(3), 207–221 (2001)
5. Banerjee, M., Ghorai, S., Mukherjee, N.: Study of cross-diffusion induced Turing patterns in a ratio-dependent prey–predator model via amplitude equations. Appl. Math. Model. **55**, 383–399 (2018)
6. Berezovskaya, F., Isaev, A., Karev, G.: The role of taxis in dynamics of forest insects. Dokl. Biol. Sci. **365**(1–6), 148–151 (1999)
7. Berezovskaya, F., Karev, G.: Bifurcations of travelling waves in population taxis models. Phys. Uspekhi **42**(9), 917–929 (1999)
8. Cangelosi, R.A., Wollkind, D.J., Kealy-Dichone, B.J., Chaiya, I.: Nonlinear stability analyses of Turing patterns for a mussel–algae model. J. Math. Biol. **70**(6), 1249–1294 (2015)
9. Chakraborty, A., Singh, M., Lucy, D., Ridland, P.: Predator–prey model with prey-taxis and diffusion. Math. Comput. Model. **46**(3–4), 482–498 (2007)
10. Chow, S., Hale, J.K.: Methods of Bifurcation Theory. Springer, New York (1982)
11. Ding, Y., Cao, J., Jiang, W.: Double Hopf bifurcation in active control system with delayed feedback: application to glue dosing processes for particleboard. Nonlinear Dyn. **83**(3), 1567–1576 (2016)
12. Ding, Y., Jiang, W., Yu, P.: Double Hopf bifurcation in a container crane model with delayed position feedback. Appl. Math. Comput. **219**(17), 9270–9281 (2013)
13. Du, Y., Niu, B., Guo, Y., Wei, J.: Double Hopf bifurcation in delayed reaction–diffusion systems. J. Dyn. Differ. Equat. **32**, 313–358 (2020)
14. Duan, D., Niu, B., Wei, J.: Hopf-Hopf bifurcation and chaotic attractors in a delayed diffusive predator–prey model with fear effect. Chaos Solitons Fractals **123**, 206–216 (2019)
15. Ei, S.-I., Izuhara, H., Mimura, M.: Spatio-temporal oscillations in the Keller–Segel system with logistic growth. Physica D **277**, 1–21 (2014)
16. Faria, T.: Normal forms and Hopf bifurcation for partial differential equations with delays. Trans. Am. Math. Soc. **352**(5), 2217–2238 (2000)
17. Faria, T.: Stability and bifurcation for a delayed predator–prey model and the effect of diffusion. J. Math. Anal. Appl. **254**(2), 433–463 (2001)
18. Faria, T., Magalhaes, L.: Normal forms for retarded functional differential equations with parameters and applications to Hopf singularity. J. Differ. Equ. **122**, 181–200 (1995)
19. Govorukhin, V., Morgulis, A., Senina, I., Tyutyunov, Y.: Modelling of active migrations for spatially distributed populations. Surv. Appl. Ind. Math. **6**(2), 271–295 (1999)
20. Guckenheimer, J., Holmes, P.: Nonlinear Oscillations, Dynamical Systems, and Bifurcations of Vector Fields. Springer, New York (1983)
21. Hassard, B., Kazarinoff, N., Wan, Y.: Theory and Applications of Hopf Bifurcation. Cambridge University Press, New York (1981)
22. Jiang, H., Song, Y.: Normal forms of non-resonance and weak resonance double Hopf bifurcation in the retarded functional differential equations and applications. Appl. Math. Comput. **266**, 1102–1126 (2015)
23. Jiang, W., Wang, H., Cao, X.: Turing instability and Turing–Hopf bifurcation in diffusive Schnakenberg systems with gene expression time delay. J. Dyn. Differ. Equ. **31**(4), 2223–2247 (2019)
24. Jin, H.-Y., Wang, Z.-A.: Global stability of prey-taxis systems. J. Differ. Equ. **262**(3, 1), 1257–1290 (2017)
25. Kareiva, P., Odell, G.: Swarms of predators exhibit "preytaxis" if individual predators use area-restricted search. Am. Nat. **130**, 233–270 (1987)
26. Kolmogorov, A.N.: Qualitative analysis of mathematical models of populations. Prob. Cybern. **25**, 100–106 (1972)
27. Kong, L., Lu, F.: Bifurcation branch of stationary solutions in a general predator–prey system with prey-taxis. Comput. Math. Appl. **78**(1), 191–203 (2019)
28. Kuznetsov, Y.A.: Elements of Applied Bifurcation Theory. Springer, New York (1998)
29. Lee, J., Hillen, T., Lewis, M.: Pattern formation in prey-taxis systems. J. Biol. Dyn. **3**(6), 551–573 (2009)
30. Li, C., Wang, X., Shao, Y.: Steady states of a predator–prey model with prey-taxis. Nonlinear Anal. Theory Methods Appl. **97**, 155–168 (2014)
31. Losey, J., Denno, R.: The escape response of pea aphids to foliar-foraging predators: factors affecting dropping behaviour. Ecol. Entomol. **23**(1), 53–61 (1998)
32. Lotka, A.: Relation between birth rates and death rates. Science **26**, 21–22 (1907)

33. Murray, J.: Mathematical Biology II: Spatial Models and Biomedical Applications. Springer, Berlin (2003)
34. Okubo, A., Levin, S.: Diffusion and Ecological Problems: Modern Perspectives. Springer, New York (2001)
35. Painter, K.J., Hillen, T.: Spatio-temporal chaos in a chemotaxis model. Physica D **240**, 363–375 (2011)
36. Shi, J., Wang, C., Wang, H.: Diffusive spatial movement with memory and maturation delays. Nonlinearity **32**(9), 3188–3208 (2019)
37. Shi, J., Wang, C., Wang, H., Yan, X.: Diffusive spatial movement with memory. J. Dyn. Differ. Equ. **32**(2), 979–1002 (2020)
38. Song, Y., Jiang, H., Yuan, Y.: Turing–Hopf bifurcation in the reaction–diffusion system with delay and application to a diffusive predator–prey model. J. Appl. Anal. Comput. **9**(3), 1132–1164 (2019)
39. Song, Y., Shi, J., Wang, H.: Stability and bifurcation analysis in the resource-consumer model with random and memory-based diffusions. In preparation (2020)
40. Song, Y., Tang, X.: Stability, steady-state bifurcations, and Turing patterns in a predator–prey model with herd behavior and prey-taxis. Stud. Appl. Math. **139**(3), 371–404 (2017)
41. Song, Y., Wu, S., Wang, H.: Spatiotemporal dynamics in the single population model with memory-based diffusion and nonlocal effect. J. Differ. Equ. **267**(11), 6316–6351 (2019)
42. Song, Y., Zhang, T., Peng, Y.: Turing–Hopf bifurcation in the reaction–diffusion equations and its applications. Commun. Nonlinear Sci. Numer. Simul. **33**, 229–258 (2016)
43. Song, Y., Zou, X.: Spatiotemporal dynamics in a diffusive ratio-dependent predator–prey model near a Hopf–Turing bifurcation point. Comput. Math. Appl. **67**(10), 1978–1997 (2014)
44. Tao, Y.: Global existence of classical solutions to a predator–prey model with nonlinear prey-taxis. Nonlinear Anal. Real World Appl. **11**(3), 2056–2064 (2010)
45. Tello, J.I., Wrzosek, D.: Predator–prey model with diffusion and indirect prey-taxis. Math. Models Methods Appl. Sci. **26**(11, SI), 2129–2162 (2016)
46. Tsyganov, M., Biktashev, V.: Half-soliton interaction of population taxis waves in predator–prey systems with pursuit and evasion. Phys. Rev. E **70**(3), 031901 (2004)
47. Tyutyunov, Y., Titova, L., Arditi, R.: A minimal model of pursuit-evasion in a predator–prey system. Math. Model. Nat. Phenom. **2**(4), 122–134 (2007)
48. Tyutyunov, Y., Sen, V.D., Titova, L., Banerjee, I.M.: Predator overcomes the Allee effect due to indirect prey-taxis. Ecol. Complex. **39**, 100772 (2019)
49. Tyutyunov, Y.V., Titova, L.I., Senina, I.N.: Prey-taxis destabilizes homogeneous stationary state in spatial Gause–Kolmogorov-type model for predator–prey system. Ecol. Complex. **31**, 170–180 (2017)
50. Volterra, I.: Sui tentativi di applicazione della matematiche alle scienze biologiche esociali. G. Econ. **23**(12), 436–458 (1901)
51. Wang, J., Guo, X.: Dynamics and pattern formations in a three-species predator–prey model with two prey-taxis. J. Math. Anal. Appl. **475**(2), 1054–1072 (2019)
52. Wang, X., Wang, W., Zhang, G.: Global bifurcation of solutions for a predator–prey model with prey-taxis. Math. Methods Appl. Sci. **38**(3), 431–443 (2015)
53. Wu, S., Shi, J., Wu, B.: Global existence of solutions and uniform persistence of a diffusive predator–prey model with prey-taxis. J. Differ. Equ. **260**(7), 5847–5874 (2016)
54. Yousefnezhad, M., Mohammadi, S.A.: Stability of a predator–prey system with prey taxis in a general class of functional responses. Acta Math. Sci. **36**(1), 62–72 (2016)
55. Zhang, L., Fu, S.: Global bifurcation for a Holling–Tanner predator–prey model with prey-taxis. Nonlinear Anal. Real World Appl. **47**, 460–472 (2019)
56. Zhang, T., Liu, X., Meng, X., Zhang, T.: Spatio-temporal dynamics near the steady state of a planktonic system. Comput. Math. Appl. **75**(12), 4490–4504 (2018)
57. Zuo, W., Wei, J.: Stability and Hopf bifurcation in a diffusive predator–prey system with delay effect. Nonlinear Anal. Real World Appl. **12**(4), 1998–2011 (2011)